Report Number 94-09

Research

Investigation of Large-Stone Mixtures

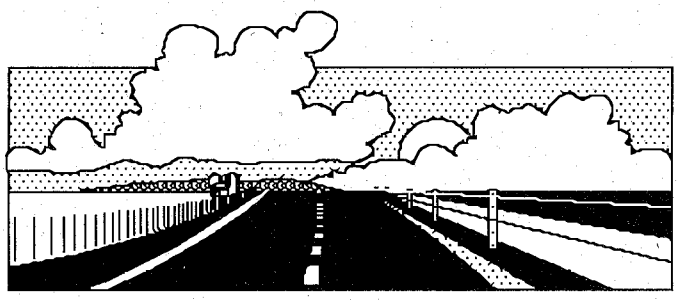

DENSE GRADED MIX

OPEN GRADED MIX

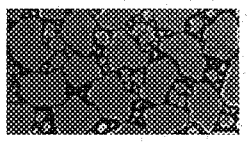

STONE FILLED MIX

UNIVERSITY OF MINNESOTA

CENTER FOR
TRANSPORTATION
STUDIES

Report Documentation Page

1. Report No.	2.	3. Recipient's Accession No.
MN/RC - 94/09		

4. Title and Subtitle	5. Report Date
Investigation of Large-Stone Mixtures	December 1993
	6.

7. Author(s)	8. Performing Organization Report No.
David E. Newcomb, Zhang Wei, Mary Stroup-Gardiner	

9. Performing Organization Name and Address	10. Project/Task/Work Unit No.
Civil & Mineral Engineering Department University of Minnesota 500 Pillsbury Dr. SE Minneapolis, Mn 55455	11. Contract(C) or Grant(G) No. (C) Mn/DOT 68893 TOC 76

12. Sponsoring Organization Name and Address	13. Type of Report and Period Covered
Minnesota Department of Transportation Office of Research Administration 200 Ford Building-Mail Stop 330 117 University Avenue St. Paul, Mn. 55155	Final Report 1992-1993
	14. Sponsoring Agency Code

15. Supplementary Notes

16. Abstract (Limit: 200 words)

This report presents the results of a one-year study on large-stone asphalt mixtures (LSAM). A thorough review of the existing technology regarding materials, mix design, and performance is included. This study expanded upon the body of knowledge by exploring an easier means of mixture design and explaining the fundamental properties of large-stone mixtures with respect to the aggregate gradation.

It was found that a dense LSAM gradation possesses better strength and durability properties than a more open LSAM gradation. Furthermore, a mix design methodology is presented wherein the optimum asphalt content for the mixture may be determined on the basis of aggregate and compacted sample properties. This eliminates the need for cumbersome Marshall stability and flow measurements. The frequency dependency of large-stone mixtures is more pronounced at low temperatures than that of a conventional mixture. The tendency for thermal cracking should be lower for a LSAM than for a conventional mixture.

Finally, recommendations are made to develop a permissive specification for LSAM, and to adopt the volumetric mixture design procedure outlined in the report.

17. Document Analysis/Descriptors	18. Availability Statement
Large-Stone Asphalt Mixtures Asphalt Mix Design Asphalt Mixture Gradation	No restrictions. This document is available through the National Technical Information Services, Springfield, Va. 22161

19. Security Class (this report)	20. Security Class (this page)	21. No. of Pages	22. Price
Unclassified	Unclassified	96	

Investigation of Large-Stone Mixtures

Final Report

Prepared by

David E. Newcomb
Wei Zhang
Mary Stroup-Gardiner

University of Minnesota
Civil and Mineral Engineering Department
500 Pillsbury Dr., S.E.
Minneapolis, Minnesota 55455

December 1993

Submitted to

Minnesota Department of Transportation
Office of Research Administration
200 Ford Building, 117 University Avenue
St. Paul, MN 55155

TABLE OF CONTENTS

List of Figures

List of Tables

EXECUTIVE SUMMARY

The concept of large stone asphalt mixtures (LSAM) has been in existence since the early 1900's. However, their use declined with the evolution of paving equipment and the advent of mix design procedures which were unsuitable for evaluating them. Recently, LSAM's have reemerged in order to combat problems with rutting in conventional dense-graded mixtures. The objective of the work presented in this report was to investigate the potential benefits of using large-size aggregate in dense-graded hot-mix asphalt. Four large-stone gradations were selected based upon information in the literature, and two of these were compared to a conventional dense-graded mixture. The LSAM's differed in terms of the proportion of the coarse aggregate.

The results showed that a modified Marshall mix design procedure could be used for determining the optimum asphalt content. Alternatively, a volumetric procedure using one set of three samples was shown to work equally well in estimating the required asphalt content. The resilient modulus frequency dependency of LSAM's was shown to be greater than that of conventional mixtures. This appeared to be a function of the specimen size and increased binder film thickness for the large-stone mixtures. The moisture sensitivity of LSAM's increased with an increasing coarseness in the aggregate gradation for mixtures containing approximately an equal volume of air voids. However, it is suggested that the asphalt content be increased in coarser mixtures to avoid this problem in the field. It was noted that the use of LSAM's may reduce problems with thermal cracking based upon the results of slow-load indirect tensile testing at low temperatures.

It is recommended that a permissive specification be developed to allow the use of LSAM's. The densest gradation used in this study is recommended as a guideline for establishing the specification. The volumetric method of mix design is recommended for

determining the optimum asphalt content of LSAM's. Finally, LSAM's would probably work best in base or binder courses in pavements.

CHAPTER ONE

INTRODUCTION

Background

Any asphalt concrete mixture with a top aggregate size greater than 25 mm (1 in.) can be called a Large-Stone Asphalt Mix (LSAM). More specifically, LSAM means those mixtures with the top aggregate size being less than 50 mm (2 in.) and at least 10 percent of the coarse aggregate with a nominal size greater than 25 mm (1 in.) (1). LSAM has been used since the 1900's when the first patent was issued to Frederick J. Warren from the Warren Brothers Co. in 1903 (2). A good understanding of the principles of bituminous pavement design was exhibited in this patent. It specified a top size aggregate of 75 mm (3 in.) which was graded for maximum density and stability. The high stability of this mixture made it possible to use a soft asphalt and to compact the mixture to less than two percent air void content. Several pavement sections placed under the Warren patent provided service to large beer wagons and trucks for over 50 years without any bleeding or rutting (2).

However, the use of large stone mixtures significantly decreased in the 1950's due to the increased use of mechanical paving equipment and the adoption of the Marshall and Hveem mixture design procedures. Both design procedures use a 100-mm (4-in.) diameter specimen which practically limits the aggregate size to 25 mm (1 in.) or less since it is generally recognized that the diameter of mold should be at least four times the nominal diameter of the coarsest aggregate in the mixture. From the construction point of view, the smaller sized aggregate produces a more workable mixture with less segregation potential.

The truck loads and tire pressures were relatively low in the 1950's and much of the cargo was transported by rail. This meant that pavements at that time were not subjected to many repetitions of heavy loads. Beginning in the early 1980's, truck loads and tire pressures increased sharply due to advances in the auto and rubber industries. For instance, on the coal haul routes in Kentucky, it was common for trucks to carry gross weights ranging from 667 to 800 kN (150,000 to 180,000 lbs) with tire pressures approaching 1034 kPa (150 psi) (1). The results were increased observations of rutting. Compare this to the fact that the current pavement design guide is based on a gross maximum weight of 356 kN (80,000 lbs) with tire pressures ranging between 621 to 724 kPa (90 to 105 psi), it is not surprising why so many pavement sections failed long before reaching the end of their design lives. Due to this circumstance, LSAM gained the attention of asphalt technologists again due to its recorded performance in resisting heavy truck loads. Many states, including Kentucky, Iowa, and Pennsylvania tried to increase the stiffness of asphalt concrete by increasing the top size of aggregate and/or the percentage of crushed stone in the mixture. The idea behind this was to change the basic load carrying structure of the mixture so that the traffic was supported by direct stone to stone contact. The initial results looked promising and research programs were begun to investigate mix design procedures and methods of estimating fundamental pavement properties.

Objective

The objective of this work was to investigate the potential benefits of using large-size aggregate in dense-graded hot-mix asphalt.

Scope

This research project will provide an initial laboratory characterization of asphalt mixtures containing large maximum size aggregate. Four large-stone gradations were selected based on the information from literature. Two large-stone mixtures were compared to a conventional dense-graded mixture. In this study, the sources of asphalt and aggregate are constant. The two large-stone mixtures differ in terms of the proportion of the maximum aggregate size.

Report Organization

Chapter one gives a brief overview of background of LSAM, the motivation of conducting the laboratory investigation, the objective of such an investigation, and the scope of the investigation. Chapter 2 summarizes detailed information about LSAM described in available literatures. Chapter 3 describes the laboratory experimental design plan and the material properties. Chapter 4 details the sample preparation and testing procedures. Chapter 5 explains the conventional Marshall mix design and volumetric mix design results. Chapter 6 summarizes all the laboratory testing results. Derivations of the theoretical formulae for diametral and uniaxial compression tests are given in Appendix A.

CHAPTER TWO

LITERATURE REVIEW

A literature search was conducted in order to:

1. Summarize the current practice and research of LSAM in both the United States and Europe.
2. Identify the effectiveness of LSAM in reducing rutting on heavily trafficked asphalt pavements.
3. Provide sufficient information for designing a reasonable laboratory testing plan to evaluate the fundamental characteristics of LSAM.

This literature research evaluated all available technical reports and papers published in the last five years about LSAM. Information was obtained on the history of LSAM usage, critical material properties, mix design practices, laboratory testing, and field experiences.

Types of LSAM Gradations

LSAM can be divided into three categories (Figure 2-1), namely dense graded mix, stone-filled mix, and open graded mix according to the load carrying mechanism (3). The dense graded mix develops strength from aggregate interlock and binder viscosity. It is characterized by high stability and the air void content is typically between 4 and 8 percent. The stone-filled mix uses a small top size asphalt concrete mix combined with larger single sized stones of up to 38 mm (1.5 in) for base courses and a smaller sized stone for surface courses. It develops

strength by an aggregate bridging effect. An open graded mix consists of large top size crushed stone (up to 64 mm (2.5 in)), low asphalt content (typically 2.0 percent) and void contents between 15 to 30 percent. It develops strength from direct stone contact and is characterized by high permeability.

Influence of Material Properties

The material properties of asphalt concrete usually include the resilient modulus, indirect tensile strength, creep compliance, and the freeze and thaw characteristics. Asphalt concrete consists of coarse aggregate, fine aggregate, asphalt, and/or additives. All these components affect the material's properties to some degree. In addition, the properties of asphalt concrete also depend on the mixing and compacting method. In research practice, emphasis is put on the influence of aggregate properties and binder properties under given mixing and compacting methods. A variety of research programs have shown that critical LSAM mixture properties are usually related to aggregate properties. Little influence on LSAM properties by changes in either binder grade or content was noted in the literature.

Coarse Aggregate

Coarse aggregate can be characterized by its type, top size, and the gradation. The percentage of crushed particles influences the mixture's compressive strength, resistance to permanent deformation, and mix design parameters such as Marshall stability. Increasing the percentage of crushed particles in asphalt mixture can yield a substantial increase in Marshall stability. With 30 percent of crushed aggregates, the increase in stability is approximately 1.8 kN (400 lb) for each additional 10 percent of crushed aggregate (4). However,

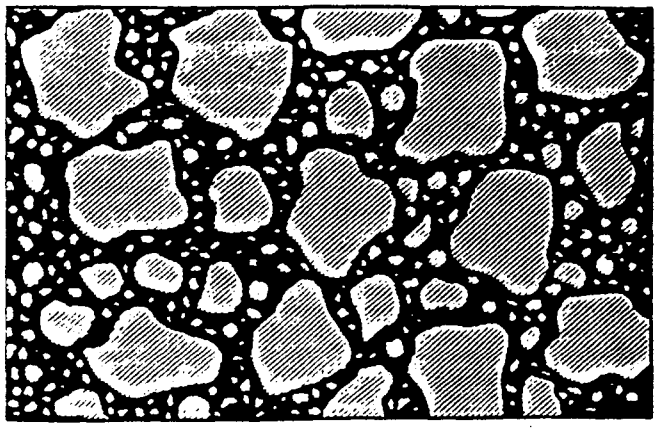

(a). Dense graded mix

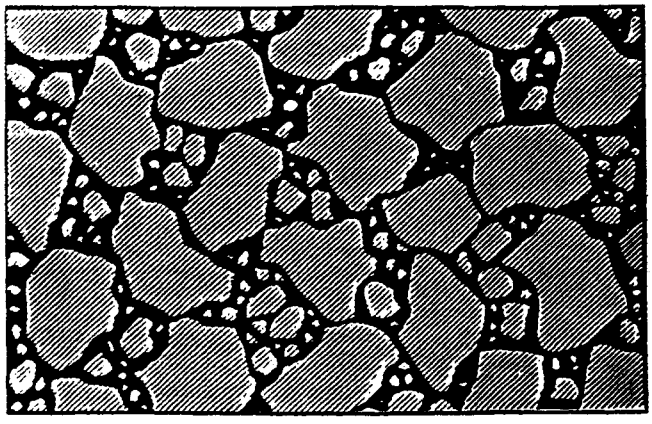

(b). Stone-filled mix

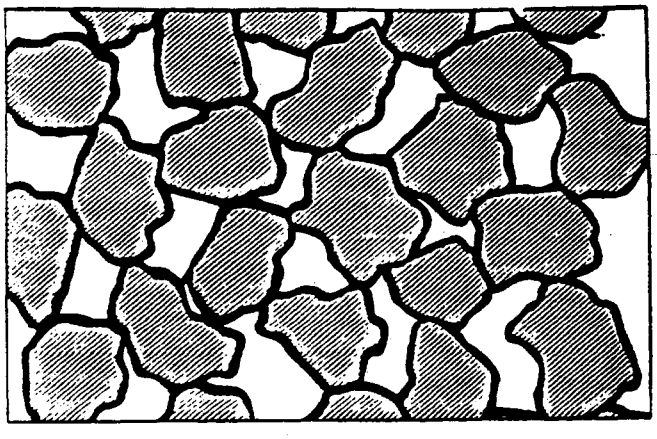

(c). Open graded mix

Figure 2-1. Types of Large Stone Asphalt Mix (3)

if the proportion of crushed particles is over 60 percent, a further increase in crushed particles will yield little additional increase in the stability (4). The creep resistance of asphalt concrete depends heavily on the proportion of crushed aggregate; as the percentage of crushed aggregate is increased, so is the mixture's resistance to rutting (4). Research has shown that the type of aggregate is also important. When the proportion of crushed aggregate is 60 percent, crushed limestone can yield stabilities as much as 40 percent higher than crushed gravel or crushed quartzite (4).

Increasing the maximum aggregate size increases the resilient modulus of asphalt concrete which means that mixes with increased maximum aggregate size are stiffer and thus should reduce stresses in the underlying layers (5, 6). Increasing the maximum aggregate size also reduces the permanent deformation of asphalt concrete under constant or dynamic loading. This indicates that increasing the maximum aggregate size will increase the rutting resistance of asphalt concrete (5, 6). Larger top size aggregates also mean that the size of the specimen will need to be increased to stay within the guidelines of a specimen diameter at least four times greater than the maximum size of aggregate. For mixtures containing aggregate with a top size larger than 25 mm (1 in) but smaller than 38 mm (1-1/2 in), a 150 mm (6 in) mold should be used for laboratory mix design.

Kandhal found that when the specimen size is increased, the compactive effort will also have to be adjusted so that a comparable density is obtained. To obtain an equivalent compaction level, the number of blows needed for an 150 mm (6 in) specimen should be 1.5 times that of an 100 mm (4 in) specimen. For example, if 50 blows were used to compact the 100 mm (4 in) specimen, then to achieve the same level of compaction, 75 blows should be

used for 150 mm (6 in) specimen (7, 8). This increase in specimen size is important; using too small of a specimen can result in inaccurate conclusions, or variable test results. Research has shown that the 150 mm (6 in) specimen for a given LSAM gradation generally showed improvement in mix properties as the maximum aggregate size increases, whereas the 100 mm (4 in) specimen generally showed an opposite trend (5). Using the 100 mm (4 in) diameter specimens would therefore lead to an illogical conclusion. For the same testing, the 150 mm (6 in) specimens were less variable than those for the 100 mm (4 in) specimens.

Asphalt Cement: The percentage of asphalt cement in the mixture has a minimal effect on stabilities until there is an excess of asphalt cement. Generally, there is a loss of stability only after the asphalt cement content exceeds 6 percent (4). Increasing the viscosity of the binder has only a minimal effect on stabilities; there is a slight increase in stabilities with increasing binder viscosity.

The binder grade, however, has a profound effect on the resilient modulus and indirect tensile strengths of these mixtures (4). Table 2-1 shows the results based on limestone mixtures.

Table 2-1. Material Properties Affected By Asphalt Grade (4)

Asphalt Grade	Material Properties MPa (ksi)	
	Resilient Modulus	Indirect Tensile Strength
AC 2.5	1400 (200)	0.49 (70)
AC 10	3143 (450)	0.98 (140)
AC 20	6287 (900)	1.19 (170)

Mix Design Practices

The conventional Marshall mix design procedure (ASTM D1559) for flexible pavement specifies the use of a 100 mm (4 in) diameter specimen mold for mixes containing aggregate up to 25 mm (1 in) maximum size, the compaction hammer weighs 4.5 kg (10 lb) and has a free fall distance of 457 mm (18 in). This procedure cannot be used for designing asphalt concrete mixes in which the maximum permissible aggregate size is greater than 25 mm (1 in), since the diameter of the mold should be at least four times the nominal diameter of the coarsest aggregate in the mixture .

In 1969, the Pennsylvania Department of Transportation (Penn DOT) started a research project on LSAM due to their special needs to design a binder course mix and base course in which the specified maximum aggregate sizes were 38 and 51 mm (1-1/2 and 2 in) respectively (7). The first set of equipment for preparing 150 mm (6 in) diameter specimens and the first tentative standard for a modified Marshall mix design procedure using a 150 mm (6 in) specimen were developed by Penn DOT in 1970 (7). After a series of compaction tests on conventional mixtures, it was decided that the nominal height of the 150 mm (6 in) diameter specimen be set to 95 mm (3.75 in) to maintain the same diameter/height ratio used for the conventional 100 mm/63 mm (4 in/2.5 in) specimen. When designing the compactor, it was assumed that the weight of the hammer should be increased in proportion to the top surface area of the specimen, the drop distance of the hammer and the number of blows on the each side of the specimen remain the same. Therefore the hammer weight was increased from 4.5 kg (10 lb) to 10.2 kg (22.5 lb), and the hammer drop height was maintained at 457 mm (18 in), with 50 blows on each side. However, the initial test data indicated that the energy input to the specimen during

compaction should have been based on energy input per unit volume instead of per unit surface area.

Let $E = M\ g\ H$ be the input energy per blow

$V = 1/4\ \pi\ D^2\ h$ be the volume of the sample

N the number of blows per side of the sample

Assuming equivalent unit volume energy input for 100 mm (4 in) and 150 mm (6 in) specimen,

$$\frac{E_1}{V_1} = \frac{E_2}{V_2} \quad \text{or} \quad \frac{N_1 M_1 g H_1}{\frac{1}{4}\pi D_1^2 h_1} = \frac{N_2 M_2 g H_2}{\frac{1}{4}\pi D_2^2 h_2} \tag{2-1}$$

$$N_2 = N_1 \frac{M_1 g H_1}{M_2 g H_2} \frac{D_2^2 h_2}{D_1^2 h_1} = N_1 \frac{10*18}{22.5*18} \frac{6^2*3.75}{4^2*2.5} = 1.5N_1 \tag{2-2}$$

Where:

N = number of blows per side

M = mass of the hammer, kg (lb)

g = acceleration due to gravity, 9.81 m/s^2 (32.2 ft/s^2)

H = drop height, mm (in)

D = sample diameter, mm (in)

h = sample height, mm (in)

Subscript "1" denotes 100 mm (4-in) specimen

Subscript "2" denotes 150 mm (6-in) specimen.

Based on this equation used to obtain the same unit volume energy input, the number of blows per side were increased from 50 to 75.

At least three samples for each combination of aggregates and asphalt contents should be prepared and tested (7, 8, 9). In order to achieve sufficient density and yet leave room for further densification under traffic, the optimum asphalt content should be set based on 4.5 ($\pm$ 1.0) percent air voids under a given compaction effort (7, 8). The mixing and compacting temperatures should be set at the temperatures that will yield a viscosity of 170 ($\pm$20) cSt and 280 ($\pm$ 30) cSt, respectively (7, 8). Table 2-2 lists the acceptable criteria adopted by Kentucky Department Of Highway (Ken DOH). For mixes containing aggregates with a top size larger than 25 mm (1 in), 150 mm (6 in) diameter specimens should be used, and 75 or 112 compaction blows on each side of the specimen should be applied depending on the anticipated field traffic. Laboratory tests for a modified Marshall design procedure of LSAM include the standard mix design tests (stability, flow, air voids, VMA) as well as adding the determination of moisture sensitivity using a ratio of retained tensile strength. Antistripping additives may be required to reduce moisture sensitivity but are not mandatory.

Table 2-2. Acceptable Criteria for LSAM (Ken DOH) (7)

Property	Requirement
Stability	13.3 kN(3,000 lb) minimum
Flow	28 maximum
VMA	11.5 percent minimum
Air void	4.5+/-1.0 percent
Retained Tensile Strength	70% minimum

Specifications

The only materials specifications found in the literature address the aggregate gradations. Tables 2-3 and 2-4 are the LSAM gradation bends recommended by Penn DOT and the Ken DOH respectively (7, 10). Both specifications indicate that the coarse aggregate should be crushed stone or crushed slag; gravel should not be permitted (7). Fine aggregate should be crushed sand or a blend of crushed sand and natural sand. Natural sand alone should not be permitted (7).

Potential Benefits and Problems

The benefit of using LSAM gradations is that they can effectively reduce the rutting of pavement under heavy truck loads and increase its service life. It is one of the few alternatives available at this time to counteract the effect of heavy truck loads and high tire pressures. The idea of using LSAM is to change the basic structure of asphalt concrete and shift the load carrying path from the weak asphalt mortar to the strong aggregate direct contact so the mix does not depend on the asphalt or the mastic for shear strength. LSAM is suitable for full depth pavement and requires less aggregate processing.

Potential problems associated with LSAM include segregation during compaction and excessive wear of paving equipment (11). Most large stone asphalt mixes are susceptible to segregation and are difficult to compact. A thicker film (9 to 11 microns) is desirable to assist compaction and a longer plant mixing time is necessary to ensure coating of larger aggregate particles (11). Segregation problem can be minimized by using multiple material drops and limit the lift thickness to greater than 3.5 in. during construction (11).

Table 2-3. Penn DOT LSAM Gradation Bend (8)

	Nominal Maximum Size of Aggregate		
Sieve Size	51 mm (2 in)	38 mm (1.5 in)	25 mm (1 in)
62.5 mm (2 1/2 - in)	100	...	...
50 mm (2 - in)	90-100	100	...
38.1 mm (1 1/2 - in)	...	90-100	100
25 mm (1- in)	60-80	...	90-100
19 mm (3/4 - in)	...	56-80	...
12.5 mm (1/2 - in)	35-65	...	56-80
9.5 mm (3/8 - in)	...	...	...
4.75 mm (No. 4)	17-47	23-53	29-59
2.36 mm (No. 8)	10-36	15-41	19-45
0.3 mm (No. 50)	3-15	4-16	5-17
0.075 mm (No. 200)	0-5	0-6	1-7

Table 2-4. Kentucky K Base Gradation Bend (10)

Sieve Size	% Passing
50 mm (2 - in)	100
38.1 mm (1 1/2 - in)	85-100
25 mm (1- in)	67-90
19 mm (3/4 - in)	56-80
12.5 mm (1/2 - in)	43-72
9.5 mm (3/8 - in)	37-60
4.75 mm (No. 4)	22-45
2.36 mm (No. 8)	14-35
1.18 mm (No. 16)	8-25
0.6 mm (No. 30)	6-18
0.3 mm (No. 50)	4-13
0.15 mm (No. 100)	3-9
0.075 mm (No. 200)	2-6

Few changes in current construction practices seem to be indicated. In Kentucky, the hot mix time was extended to 25 to 30 seconds, the compaction temperature was set between 121^{0}C (250^{0}F) and 149^{0}C (300^{0}F). The required density was achieved using conventional compaction equipment. Wearing of paving equipment was not obvious.

European Experience

The European roadway system experienced a similar problem with permanent deformation. The European asphalt technologists have developed several types of special purpose asphalt mixes to counteract this problem. Among them are the Stone Mastic Asphalt (SMA) developed in West Germany in the 1960's, the Hot Rolled Asphalt developed in England, the Gussasphalt developed in France, and the Porous or Drainage Asphalt developed in Sweden (12). Many pavement sections in the European countries placed using these special purpose asphalt mixes have been subjected to heavy truck loads for more than ten years, and are still in excellent service condition.

Stone Mastic Asphalt (SMA) is a gap-graded mix using single top size aggregate (16 to 22 mm (5/8 to 7/8 in)) and mastic (asphalt cement plus fine aggregate (less than 2 mm) and filler). Additives such as rock wool and short cellular fibers are usually used to prevent the fine particles from being drained away from the mixture during construction. It relies on the direct stone contact for high strength. In the German Technical Specification, SMA mixes are generally called Splittmastixasphalt. Like LSAM, the idea of SMA is also to form a strong stone skeleton to support the traffic, but it adopts a difference approach. Instead of using a large top size (larger than 25 mm (1 in)) dense graded aggregate, it uses a small top size (16 mm (5/8 in))

gap graded aggregate with a high filler content and a high asphalt content. The characteristics of SMA include:

1. Using a high content of crushed gap-graded coarse aggregate to achieve high stability and to reduce densification under traffic through excellent particle interlock (14).
2. Using coarse premium aggregates with high content of traprock diabus to achieve high wear resistance (14).
3. Using high asphalt content (with soft asphalt) to produce a voidless mastic mortar which can partly fill the voids in the stone skeleton and bond the aggregate together. Thus ensures longevity and durability to premature cracking, ravelling, and stripping (14).
4. Using stabilizing additives to improve homogeneity and stability and prevent segregation during mixing, transportation, and paving (14).

Surprisingly, limestone which is considered the best paving aggregate in some parts of the United State is rarely used in Germany due to its lower strength. Modifiers that have been used include cellulose fibers, rubber crumbs, synthetic silica and various polymer additives. The purpose of using modifiers is to stiffen the asphalt cement to prevent binder run-off during mixing, transportation, and lay down operation.

More attention was paid to material selection and performance specification in the European paving industry. The coarse aggregates were usually imported high quality materials. At least 50 percent of the fine aggregate must be crushed sand. Should any defect or distress occur within the warrantee period (1 to 4 years), the contractor must repair it at his own expense

in accordance with the contract provisions. Usually SMA costs 20 percent more than conventional HMA, but its service life is twice as long.

Summary

Rutting resistance can be improved by increasing the top size and the proportion of crushed coarse aggregate. The improved performance of a properly designed LSAM is due to the fact that it can produce an interlocked aggregate framework which does not depend on the asphalt or mastic for shear strength. Since the introduction of LSAM is aimed at changing the load carrying structure of asphalt concrete, new design procedures need to be developed which can better simulate the field condition and thus better predict the field performance.

Because of the limited amount of data found in the literature, more information needs to be collected in order to better understand the mechanisms of LSAM; additional emphasis is needed on defining the creep and repeated loading behavior.

CHAPTER THREE

EXPERIMENTAL DESIGN AND MATERIALS

Experimental Design

Based upon the information obtained from the literature search, a full one factor experiment with five levels was designed to meet the objectives of this research program (Table 3-1). The single factor under consideration was the aggregate gradation. Four of the five levels were LSAM gradations (described fully in the Materials section); the fifth level represented the conventional dense graded paving mixtures.

This design was used to investigate four areas of mixture properties: temperature susceptibility, moisture sensitivity, low temperature behavior, and permanent deformation characteristics. The large stone mixes were designated LSAM-1 through LSAM-4. The mixture designated LSAM-1 represented the coarsest gradation, and LSAM-4 had the highest proportion of fines. The LSAM-1 gradation was removed from the experimental design during the mix design portion of the program due to persistent problems with segregation. The LSAM-3 was also removed from the experimental design after mix designs were completed as results for this mixture consistently fell between those for the LSAM-2 and LSAM-4. It was felt that an evaluation of the LSAM-2 and LSAM-4 would therefore bracket any results that would be obtained for the LSAM-3.

Table 3-1. Experimental Design

Asphalt Cement	Gradations				
	Type 41 Control	LSAM-1	LSAM-2	LSAM-3	LSAM-4
85/100	ABCD		ABCD		ABCD

A: Temperature susceptibility, 4 temperatures, 3 replicates (3 samples/gradation)
B: Moisture sensitivity, 3 replicates (3 samples/gradation)
C: Low temperature behavior , 1 strain rate, 2 temperatures, 2 replicates (4 samples/gradation)
D: Permanent deformation, 1 temperature, 2 deviator stresses, 2 replicates (4 samples/gradation)

Materials

Asphalt Cement

Since the literature review indicated that the grade of binder had only a minimal impact on LSAM mixture properties, only one binder was used throughout the research program. This was an 85/100 penetration graded binder supplied by Koch Refinery of Inver Grove Heights, Minnesota; this binder is one of two grades commonly used in Minnesota. Limited physical properties are shown in Table 3-2.

Table 3-2. Physical Properties of Asphalt Cement

Properties	85/100 Pen Asphalt Cement	
	Original	After Rolling Thin Film Oven Test
Original Viscosities:		
60°C, Poise	1,588	5,372
135° C, cSt	362	558
Original Penetration, 25°C, 0.1dmm	89	NA

Aggregate

Five gradations were selected: one typical 2331 Type 41 Mn/DOT dense gradation (control), and four LSAM gradations (Table 3-3, Figure 3-1). The Type 41 gradation used represents the middle of the Mn/DOT 2331 Type 41 gradation specification band. The LSAM gradations were selected based upon the literature review; the Kentucky K-base gradation was used as a starting point for these gradations. Variations in the LSAM gradations were limited to changes in the 4.75 mm (No. 4) and above fractions so that the influence of increasing the percentage of large aggregate in a given gradation could be evaluated. The coarse aggregate fractions (i.e., No. 4 and above) were held constant at 67 percent of the gradation. The percentage of the 25 mm (1-inch) aggregate fraction varied from 32 percent for LSAM-1 to 10 percent for LSAM 4.

The Type 41 gradation was prepared from three aggregate sources. The 9.5 mm (3/8-inch) fraction was obtained from Meridian Inc., Granite Falls, Minnesota quarry and was a 100 percent crushed granite. The 4.75 mm (No.4) through 0.075 mm (No. 200) aggregate fractions were obtained from the Commercial Asphalt, Inc., Lakeland, Minnesota quarry and was a partially crushed river gravel. The physical properties of all aggregate sources are shown in Table 3-4. The minus 0.075 mm (No. 200) material was bag house fines obtained from Commercial Asphalt, Inc. St. Paul, Minnesota plant.

The bag house material was initially substituted for the minus 0.075 mm (No. 200) Lakeland because of difficulty in sieving a sufficient quantity of this material. Table 3-5 shows that there was a significant difference in the properties of the fine materials. Where the Lakeland minus 0.075 mm (No. 200) was non-plastic, the bag house fines had a plasticity limit of around

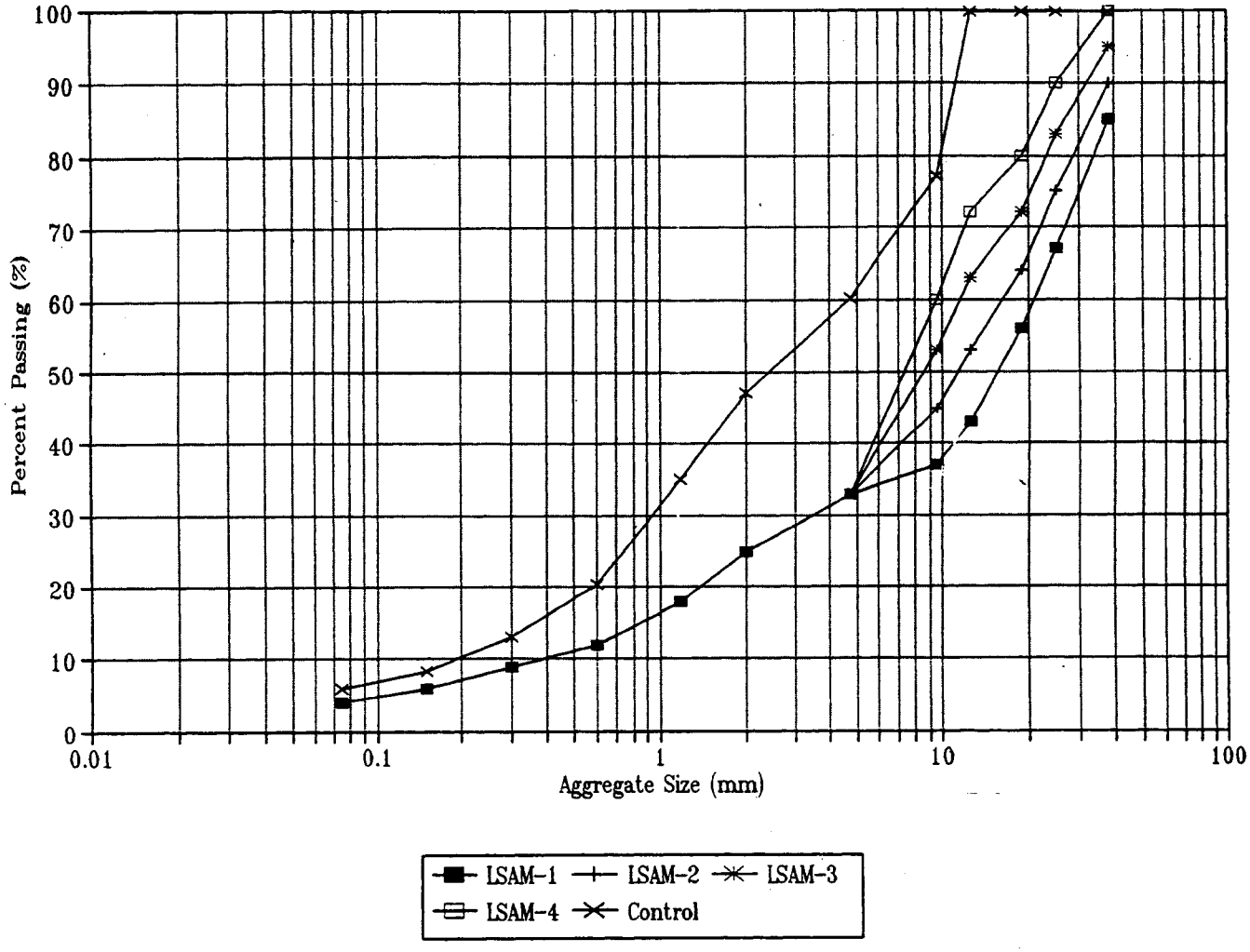

Figure 3-1. Aggregate Gradations

22 percent. Also, the bag house material was considerably finer than the Lakeland. While there was a significant difference in the two materials, it was felt that because of the low percentage of minus 0.075 mm (No. 200) in the mixtures this should not cause a problem as the plasticity limit for the combined fines was estimated to be below 2 percent. Generally, fines are considered non-plastic in the range of 0 (i.e., NP) to 4 percent.

The LSAM gradations were prepared with the same three sources of aggregates as the control gradation. The crushed granite was used for the 38 mm (1-1/2-inch) through 9.5 mm (3/8-inch) fractions, the partially crushed river gravel for the 4.75mm (No. 4) through 0.075 mm (No. 200) fractions, and the bag house fines for the minus 0.075 mm (No. 200). Differences between the four LSAM gradations were confined to variations in the 4.75 mm (No.4) and above fractions; the fine aggregate (i.e, minus 4.75 mm (No.4)) gradation was held constant for all of the mixtures.

Table 3-3. Aggregate Gradations

Sieve Size	Cumulative Percent Passing, %				
	Control	LSAM-1	LSAM-2	LSAM-3	LSAM-4
25 mm (1-in)	100	67	75	83	90
19 mm (3/4-in)	100	56	64	72	80
12.5 mm, (1/2-in.)	100	43	53	63	72
9.5 mm (3/8-in)	77	37	45	53	60
4.75 mm (No. 4)	60	33	33	33	33
2.00 mm (No. 8)	47	25	25	25	25
1.18 mm (No. 16)	35	18	18	18	18
0.60 mm (No. 30)	20	12	12	12	12
0.30 mm (No. 50)	13	9	9	9	9
0.15 mm (No. 100)	8	6	6	6	6
0.075 mm (No.200)	6	4	4	4	4

Table 3-4. Aggregate Physical Properties

Properties	Crushed Granite (+No. 4) and Lakeland (No.4) (Coarse Agg.)				Partially Crushed River Gravel (Fine Agg.)
	LSAM-1	LSAM-2	LSAM-3	LSAM-4	
Bulk Specific Gravity	2.634	2.628	2.621	2.615	2.582
Bulk Specific Gravity, SSD	2.670	2.668	2.665	2.663	2.650
Apparent Specific Gravity	2.732	2.737	2.742	2.746	2.769
Absorption Capacity, %	1.3	1.5	1.7	1.8	2.6

Table 3-5. Properties of Minus No. 200 Material

Properties	Lakeland Minus No. 200	Bag House Fines[1]
Atterberg Limits		
Liquid Limit, %	19.6	35.2
Plastic Limit, %	NP	22.1
Plasticity Index, %	19.6	13.1
Hydrometer Analysis , % Finer		
Particle Size (mm) 0.0327	23.4	56
0.0210	18.3	54
0.0123	13.1	52
0.00887	10.5	49
0.00631	10.5	47
0.00314	9.0	37
0.00132	7.6	19.5

Note: Hydrometer analysis values est. from gradation graph so that a direct comparison can be made between the types of fines.

CHAPTER FOUR

SAMPLE PREPARATION AND TESTING PROGRAM

Sample Preparation

Aggregate from individual sized stockpiles were batched to form the target gradation. Prior to mixing , the batched aggregates were dried to a constant weight in accordance with ASTM D1559, except the drying temperature was increased from 110°C (230°F) to 135°C (275°F) due to a lack of ovens. For the LSAM mixtures, one sample at a time was prepared because of the volume of material needed for one sample (4100 g/sample). A Hobart 191 (20 quart) mixer with a wire whip was used to mix the aggregate and asphalt cement. The mixtures were stored at 135°C (275°F) for three hours prior to compaction; this was per the Strategic Highway research Program (SHRP) mix design recommendation to simulate short term aging (14). The 150 mm (6-in) diameter molds were preheated at 135°C (275°F); the face of the 10.2 kg (22.5 lb) hammer was also heated on a large hot plate. The mixture was then carefully added into the mold in two layers and each layer was rodded 25 times. Some of the finer portion of the mixture was placed on the top and bottom of the mold in order to produce a smooth finished surface. This was necessary to accomplish some of the research testing which followed. A rotating base, bevel head Marshall compactor was used to compacted the samples at 75 blows per side. The samples were allowed to cool down for at least 60 minutes before being extruded from the molds.

Segregation and equipment wear problems were observed during sample preparation. Several mixer whips were broken when mixing the coarser gradations. The compacted samples

always had one side smooth and one side rough which was the result of segregation. LSAM-1 (the coarsest gradation) was abandoned in this stage because the samples disintegrated in the hot water bath (40°C (140°F)) used for conditioning the samples prior to determining the Marshall stabilities.

Two methods of preparing control samples were used. The first follows the conventional mix design procedure prescribed in American Society for Testing and Materials (ASTM) procedure D1559 (15). This method was used to prepare the standard 100 mm (4-in) diameter samples for both mix design and research testing. The above procedure outlined for preparation of the LSAM samples was also used to prepare 150 mm (6-in) diameter samples for research testing.

Creep samples were cylindrical specimens 150 mm (6 in) in diameter and 300 mm (12 in) in height and were comprised of three large Marshall samples. The samples were prepared as follows:

1. Three 150 mm (6-in) samples were prepared as described above.
2. One sample was extruded into a preheated creep mold. A thin layer of asphalt cement was used as a tack coat on top of the sample.
3. The second sample was then extruded into the mold on top of the first. Another tack coat was applied.
4. The final sample was extruded into the mold and the stacked samples were compacted by hand with ten blows using the 10.2 kg (22.5 lb) hammer. A 40 kg (88 lb) dead weight was then placed on top of the samples for at least one hour.
5. The creep sample was then extruded.

Testing Program

The research program was designed to determine the optimum asphalt cement content, then evaluate the temperature susceptibility, moisture sensitivity, low temperature behavior,and permanent deformation characteristics of the mixtures.

Mix Designs

The modified Marshall mix design as developed by Dr. Kandhal was used to determine the optimum asphalt cement content for the four LSAM gradations used in this research program (7). The Asphalt Institute Manual Series No. 2 for Mix Design Methods was followed for determining the optimum asphalt cement content for the dense graded mixtures. The Marshall stability, flow, air voids, unit weight, and VMA were determined for all mixtures.

A high load capacity hydraulic system was needed to determine the stabilities of the large stone mixtures because the loads exceeded the capacity of the load frame typically used for conventional mix designs.

Temperature Susceptibility

A closed loop servo-hydraulic MTS testing system was used to determine the resilient modulus of each sample. Since the resilient modulus test is nondestructive, each sample was tested at four temperatures starting from the coldest temperature: -18, 0, 25, and 40°C (0, 34, 77, and 104°F). Three samples were tested for each gradation.

The samples were conditioned at testing temperature for at least 24 hours before testing,

and the environmental chamber was regulated to the testing temperature for at least 10 minutes before installing the sample. The loading frequencies were set at 0.5 Hz, 1 Hz, and 2 Hz, each with 100 preconditioning cycles used for the LSAM samples. Loading frequencies of 0.33, 0.5, and 1 Hz were used for dense graded control mixtures. The larger range of loading frequencies was used for the LSAM because no information in the literature could be found regarding the frequency dependency of these mixtures. The standard frequencies specified in ASTM D4123 (16) were used for the control mixtures so that data from the 150 mm (6 in) diameter samples could be compared to previous work using the same materials prepared as 100 mm (4 in) diameter samples.

The control load varied according to the temperature; the load was selected so that the horizontal strains would be between 125 and 5000 micrometers (50 and 200 microinches). A 0.1 second loading period followed by corresponding rest period (e.g. 0.9 second rest period for a 1-Hz loading frequency) was used. Each sample was tested along in two perpendicular axes. In the data analysis, Possion's ratio was assumed to be 0.20 for either the -18°C (0°F) or 1°C (34 °F) test temperatures, and 0.35 and 0.5 for 25 and 40 °C (77 and 104 °F), respectively.

The resilient modulus for each loading frequency was determined per ASTM procedure D4123. The average total resilient modulus corresponding to each loading frequency was reported for each gradation.

Moisture Sensitivity

The ASTM procedure D4867 (17) for determining the moisture sensitivity of asphalt concrete mixtures was used; the optional freeze/thaw procedure was included in the sample

conditioning. A set of six samples was prepared for each gradation. Three samples from each set of six were taken to determine the original unconditional resilient modulus and indirect tensile strength. The remaining samples were vacuum saturated to between 55 to 80 percent, wrapped and frozen at -18°C (0°F) for 15 hours (minimum), then unwrapped and thawed in a 40°C (140°F) water bath for 24 hours. The samples were then moved to a 25°C (77°F) water bath for 2 hours to be brought to the testing temperature. The resilient moduli and indirect tensile strengths were then determined.

The resilient modulus was determined as described in the preceding section. The tensile strength was determined with a loading rate of 50 mm/min (2 in/min). Moisture sensitivity was expressed as a ratio of the wet to dry strengths. The resilient moduli and indirect tensile strengths, both before and after conditioning, the ratios, and the percent saturations achieved were reported.

Low Temperature Behavior

A constant strain indirect tension test was used to evaluate the low temperature behavior of the mixtures. Tests were conducted at -18 and 1°C (0 and 34°F); a loading rate of 0.025 mm/min (0.001 in/min) was used. The same resilient modulus testing equipment was used for indirect tension test. Samples were conditioned at a given testing temperature for at least 24 hours prior to testing. A total of six samples were prepared for each gradation (three samples per testing temperature).

The formulae used to calculate the horizontal stress and horizontal strain at the center of the specimen are as follow :

$$\sigma_t(0,0) = \frac{2P}{\pi Dt}$$

$$\epsilon_t(0,0) = \frac{\Delta H}{D}\,\frac{0.9817+2.9869\upsilon}{0.4240+1.5706\upsilon} \qquad (4\text{-}1)$$

Where:

P = applied load, kN (lb).

D = diameter of the specimen, mm (in)

t = height or thickness of the specimen, mm (in)

ΔH = total change in diameter along the horizontal axis, mm (in)

υ = Poisson's ratio

The development of the horizontal strain equation is discussed in detail in Appendix A.

Important measurements used in the analysis included the maximum tensile strength, the corresponding strain $\epsilon_r(0,0)$, and the horizontal strain energy at failure. The horizontal strain energy was defined as the area under the $\sigma_r(0,0)$ versus $\epsilon_r(0,0)$ curve.

Permanent Deformation Characteristics

The static triaxial creep test was conducted at 40°C (104°F) with a 207 kPa (30 psi) confining pressure. Four creep samples were prepared for each gradation. Two samples from each set of four were tested under a 104 kPa (15 psi) deviator stress, the remaining samples were tested under a 311 kPa (45 psi) deviator stress.

A rubber membrane was placed over each creep sample, and then conditioned at 40°C (104°F) for 24 hours prior to testing. The sample was then placed on the bottom platen in a

triaxial chamber, the top platen was added and the membrane sealed around the platens. The top platen was fitted with two LVDT's 180° apart, and the chamber was sealed and pressurized. This configuration measured the full axial displacement. An MTS closed loop system was used to control the test while the MTS Testar program was used to acquire the data. The creep samples were preconditioned under a given deviator stress for two minutes, followed by a 2 minute rest period, then reloaded with the designated deviator stress for one hour. At the end of 1 hour, the load was removed and the recoverable deformation was measured for 20 minutes.

The data collected from this testing sequence was used to calculate key Burger model parameters (discussed in Appendix A), such as creep compliance and creep modulus.

CHAPTER FIVE

MIX DESIGNS

Both the Marshall mix design for the conventional size samples (control samples only) and modified Marshall mix design (LSAM only) for the large diameter samples were completed. Because the modified design for the LSAM requires large quantities of materials, specialized equipment, and longer sample preparation and testing times, two volumetric mix designs approaches were also explored.

Marshall Mix Design

The results from the mix design work for the LSAM are shown in Table 5-1 and Figure 5-1. The optimum binder content was selected based on 4 percent air voids. Figure 5-1 shows that for any given asphalt content, the properties of the LSAM-3 (intermediate LSAM gradation) generally fell between LSAM-2 (coarsest LSAM gradation) and LSAM-4 (finest LSAM gradation). As the gradation became coarser (from LSAM-4 to LSAM-2) the optimum binder content decreased. Table 5-2 summarizes the mix design parameters for each gradation at the optimum binder content as well as the results from the control mix design (100 mm (4 in) samples). At the optimum binder content (Table 5-2), the VMA decreased as the gradation became coarser; there was little change in the unit weight, stability, or flow.

Table 5-1. Average Modified Marshall Mix Design Results (150 mm (6-in) Diameter Samples)

Asphalt Content (Total Wt. Mix)	Marshall Stability kN (lb)	Marshall Flow mm (0.01 in)	Air Voids, %	VMA, %
LSAM - 2 (Coarsest)				
2.9	20.6 (4,632)	3.05 (12)	4.5	13.3
3.4	18.9 (4,254)	3.56 (14)	3.8	13.3
3.9	18.6 (4,183)	3.30 (13)	2.	13.1
4.3	21.9 (4,932)	3.81 (15)	1.4	12.7
LSAM -3				
2.9	22.4 (5,029)	3.05 (12)	5.9	14.4
3.4	25.6 (5,745)	3.81 (15)	4.4	14.2
3.9	20.4 (4,582)	3.56 (14)	6.7	14.0
4.3	24.5 (5,501)	4.32 (17)	2.8	13.3
LSAM -4 (Finest)				
3.4	28.9 (6,504)	3.30 (13)	6.0	14.0
3.9	16.9 (3,805)	3.30 (13)	5.7	14.9
4.3	24.4 (5,477)	3.56 (14)	4.1	14.4
4.8	21.8 (4,895)	4.06 (16)	2.6	14.1

Table 5-2. Summary of Marshall Mix Design Results

	Control[1]	LSAM-2[2]	LSAM-3[2]	LSAM-4[2]
Air Void Contents (%)	4	4	4	4
Optimum Asphalt Content Total Wt. of Mix (%)	4.3	3.3	3.8	4.3
Unit Weight (lb/ft^3)	148.5	150	149	150
Stability (kN) (lb)	12.5 (2,800)	19.0 (4,290)	25.8 (5,790)	22.2 (5,000)
Flow (mm) (0.01 in)	2.54 (10)	3.68 (14.5)	3.56 (14.0)	3.81 (15.0)
VMA (%)	14.2	13.3	14.1	14.6

1: 100 mm (4 in) diameter samples
2: 150 mm (6 in) diameter samples

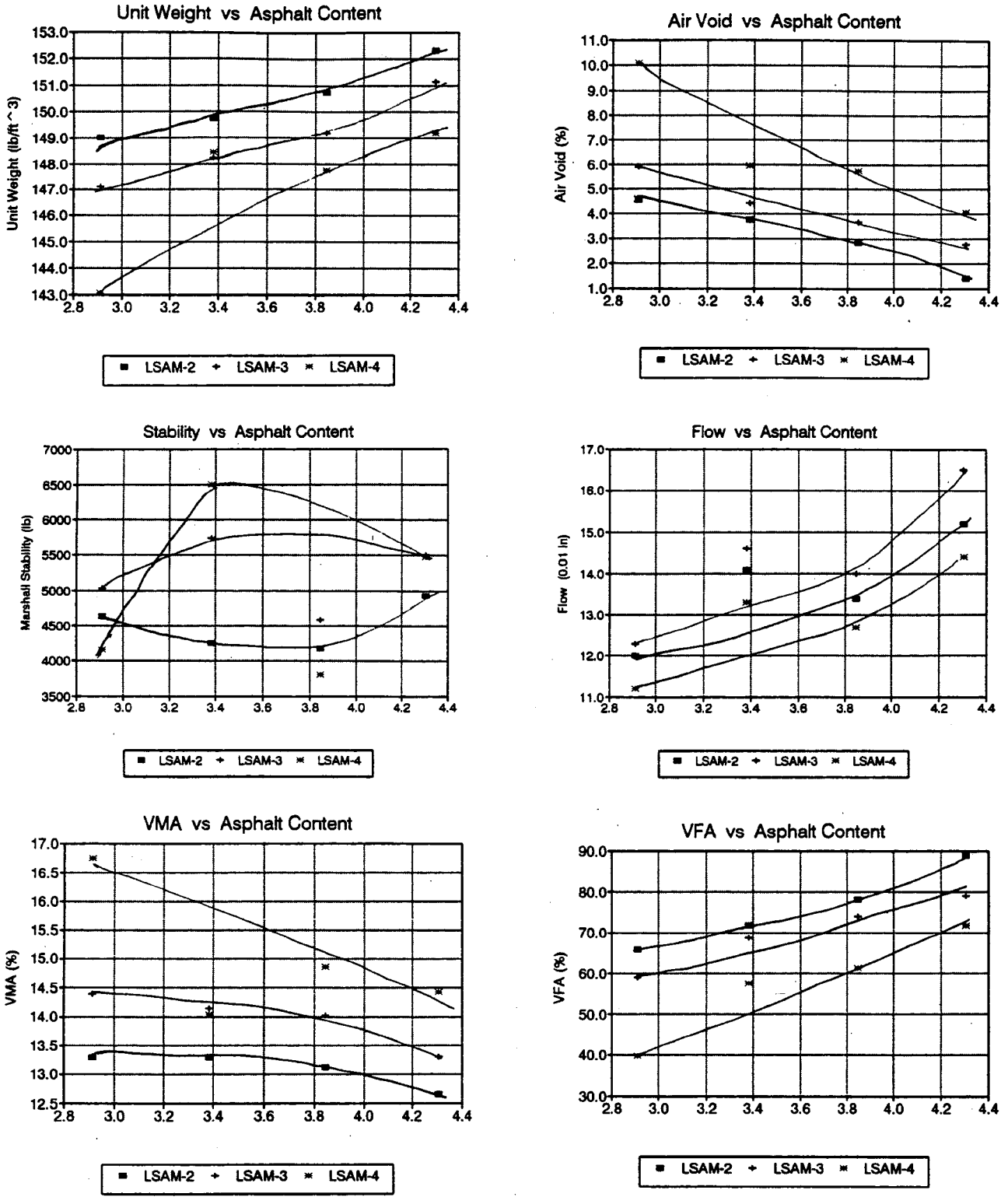

Figure 5-1. Results of Marshall Mix Design

A comparison between the control dense graded mixture and the LSAM gradations shows that the asphalt content decreased as the gradation became coarser. This is reasonable as the aggregate surface should be decreasing with the corresponding decrease in the quantity of fine aggregate. The VMA for the LSAM-3 and -4 are comparable to that for the control. The stability for the LSAM gradations are approximately double that of the control. It is possible that the difference in stabilities between control and LSAMs is as much a function of the change in sample size and test equipment as the coarseness of the gradation or the maximum top size stone.

Volumetric Mix Designs

Conducting complete Marshall mix designs for large stone mixtures requires additional capital expenditures for equipment, and larger quantities of materials. In addition, the large size of the equipment makes handling both the equipment and samples difficult and time consuming for laboratory personnel. These problems led to the exploration of two alternative mix design approaches that were less laboratory intensive.

The first alternative uses a simplistic volumetric approach which requires only the aggregate specific gravities, and the unit weight and voids for the proposed aggregate gradation. The second alternative is a slightly more complex approach and uses both aggregate and limited mixture properties. Both methods are discussed in the following sections.

Volumetric Mix Design - Based Only on Aggregate Properties

This method of determining the optimum asphalt content for a specific gradation is based on the concept shown in Figure 5-2. The steps involved in calculating the binder content are:

1. Determine the specific gravities of the aggregates (ASTM C127, C128).
2. Determine the aggregate gradation (ASTM D136).
3. Calculate the combined specific gravity for the aggregate gradation.
4. Determine the unit weight of the aggregate (ASTM C29).
5. Calculate the volume of aggregate and air voids based on the specific gravities of the aggregate (Figure 6-1).
6. Determine the specific gravity of the asphalt cement (or estimate).
7. Calculate a range of high and low asphalt contents to achieve 4 percent air voids.
8. Calculate the percent asphalt cement by total weight of mixture.

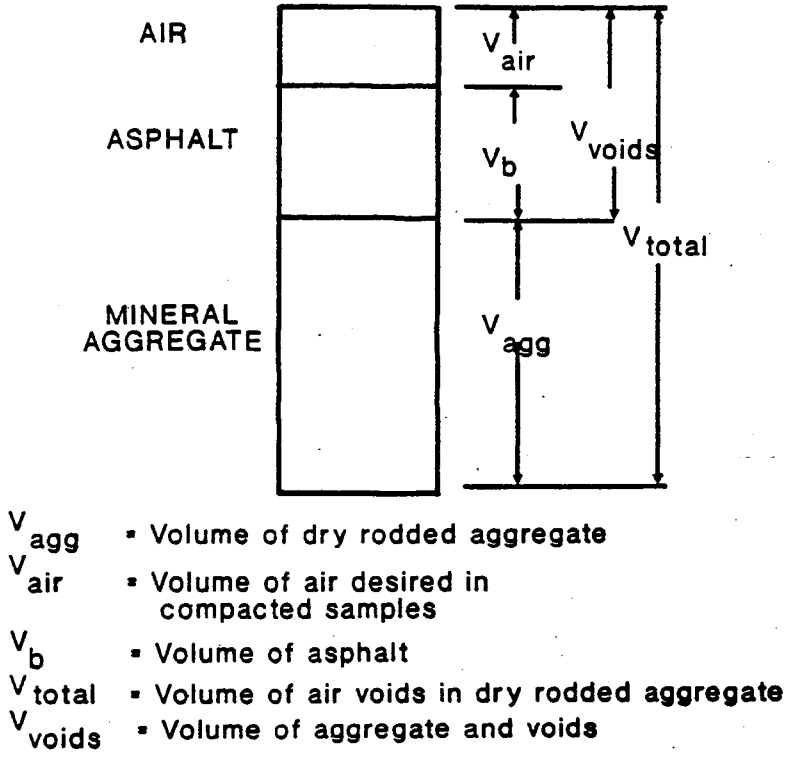

Figure 5-2. Concept of Volumetric Mix Design Based on Aggregate Properties Only (18)

The aggregate specific gravities and gradation are determined as usual. The unit weight however, is determined using the 150 mm (6-in.) Marshall mold used for compacting samples. This small volume was used because of segregation problems encountered when using a standard size unit weight bucket.

The total volume ,V_{total}, of both air voids and aggregate is calculated by:

$$V_{total} = \frac{1}{4}\pi D^2 h \qquad (5\text{-}1)$$

Where:

D = Diameter of the mold, 150 mm (6 in).

h = Height of the mold, 100 mm (4 in).

The volume of the aggregate (V_{agg}) is determined by:

$$V_{agg} = \frac{Wt_{agg}}{G_{agg}\,\gamma_{water}} \qquad (5\text{-}2)$$

Where:

Wt_{agg} = Dry rodded mass of aggregate in mold, grams

G_{agg} = Bulk or bulk saturated surface dry specific gravity of aggregate

γ_{water} = Unit weight of water (equals 1 g/cc)

The volume of air voids (V_{voids}) is:

$$V_{voids} = V_{total} - V_{agg} \qquad (5\text{-}3)$$

When the bulk specific gravity of the aggregate is used to calculate the volume of

aggregate, the volume of voids calculated will not include the surface voids in the aggregate surface. This will give a low estimate of the volume of binder needed. When the bulk specific gravity (SSD) is used, all the surface voids in the aggregate will be added to the volume of air voids. This will result in a high estimate for the volume of binder needed. The actual binder content will be between these two values as the binder will only partially absorb into the surface voids.

The required mass of binder (Wt_{AC}), in grams, is determined based on a desired level of air voids in the compacted mixture of 4 percent. The equation is:

$$Wt_{AC} = 0.94 V_{voids} G_b \gamma_{water} \quad (5\text{-}4)$$

Where:

G_b = Specific gravity of binder

V_{voids} = Volume of voids

The percent of binder by total weight of mixture is:

$$\%AC = \frac{Wt_{AC}}{Wt_{agg} + Wt_{AC}} \quad (5\text{-}5)$$

Table 5-3 shows the calculated ranges of asphalt cement contents for the four LSAM. These data show that there is a substantial difference between the calculated asphalt cement content and the content determined during mix designs. The majority of this difference is most likely the results of 1) the method used to calculate unit weights of the aggregate gradations, and 2) additional densification during compaction due to the lubricating effect of the binder.

These results indicate that this approach to estimating the asphalt cement content is not adequate.

Table 5-3 Calculated Asphalt Cement Content Using Only Aggregate Properties

Properties	Gradation			
	LSAM-1	LSAM-2	LSAM-3	LSAM-4
Bulk Specific Gravity (BSG)	2.634	2.628	2.621	2.613
Bulk Specific Gravity, SSD (BSG-SSD)	2.670	2.668	2.665	2.663
Dry Rodded Unit Weight of Aggregate (Wt_{agg}), g	3576.6	3580.2	3803.2	3683.2
Volume of Aggregate and Voids in Mold (V_{total}), cc	1959.9	1959.9	1959.9	1959.9
Volumes Based on BSG:				
Volume of Aggregate (V_{agg}), cc	1357.9	1362.9	1451.3	1408.5
Volume of Air Voids (V_{voids}), cc	602.7	597.2	508.8	551.4
Mass of AC Needed ($Wt_{AC\text{-}low}$), g	595.3	590.9	503.1	545.2
Volumes Based on BSG-SSD:				
Volume of Aggregate (V_{agg}), cc	1339.6	1341.9	1427.1	1383.1
Volume of Air Voids (V_{voids}), cc	620.3	618.0	532.8	576.8
Mass of AC Needed ($Wt_{AC\text{-}high}$), g	613.4	611.1	526.8	576.8
Low Percent AC , % by total weight of mix	14.3	14.2	11.8	12.9
High Percent AC , % by total weight of mix	14.8	14.7	12.2	13.4
Percent AC Determined in Marshall Mix Design, % (total weight of mix)	NA	3.3	3.8	4.3

Volumetric Mix Design - Based on Aggregate and Compacted Sample Properties

This method uses the concept shown in Figure 5-3. The steps are as follows:

1. Determine the bulk specific gravities of the aggregates (ASTM C127, C128).
2. Prepare 1 set of three 15 cm (6-inch) diameter samples at 4.5 percent asphalt content (dry mass of aggregate) and 2,500 g of loose mix.

3. Determine the bulk specific gravity of the compacted samples (ASTM D2726).

4. Determine the theoretical maximum specific gravity (ASTM D2041).

5. Calculate the effective specific gravity of the aggregate.

6. Calculate the voids in mineral aggregate (VMA).

7. Calculate the percent of the binder absorbed by the aggregate.

8. Calculate the binder required to produce an adequate film thickness.

9. Calculate the mass of asphalt cement needed to achieve 4 percent air voids.

10. Calculate the mass of aggregate in mixture.

11. Calculate the percent of asphalt cement by total mass of mixture.

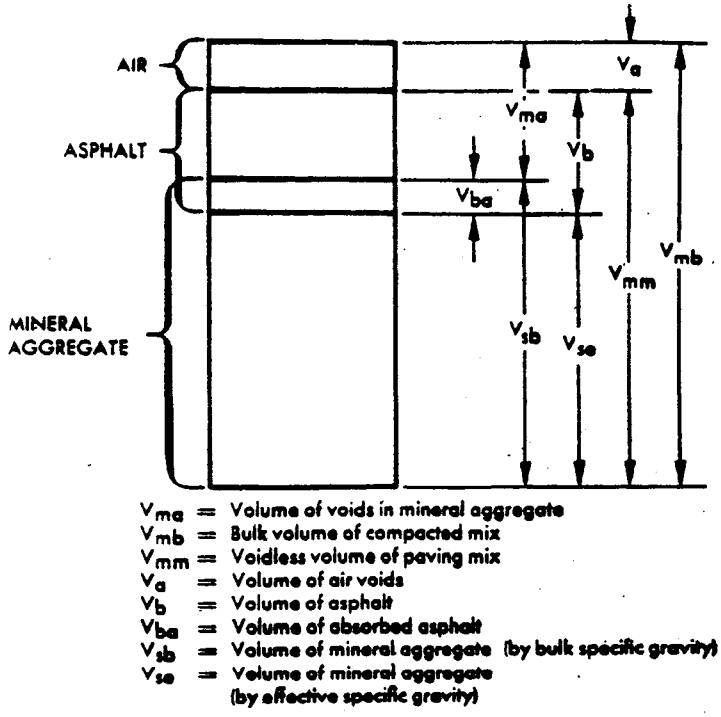

Figure 5-3. Concept of Volumetric Mix Design Based on Aggregate and Limited Compacted Sample Data (18)

The specific gravities of the aggregates and the compacted samples are determined as usual. The theoretical maximum specific gravity is used to calculate the effective specific gravity, G_{se}:

$$G_{se} = \frac{100 - P_b}{\frac{100}{G_{max}} - \frac{P_b}{G_b}} \quad (5\text{-}6)$$

Where:

P_b = Percent of binder by total mass of mixture, %

G_b = Specific gravity of binder

G_{max} = Theoretical maximum specific gravity of the mixture

The voids in mineral aggregate (VMA) includes both the air voids and the asphalt cement film thickness. The quantity of binder absorbed by the aggregate is excluded from this volume. VMA is calculated by:

$$VMA = 100 - \frac{G_{mix} P_{agg}}{G_{agg}} \quad (5\text{-}7)$$

Where:

G_{mix} = Bulk specific gravity of the compacted samples

P_{agg} = Percent of aggregate by the total weight of mixture, %

G_{agg} = Bulk specific gravity of the aggregate

The mass of binder is the sum of two calculations: the percent of the binder absorbed

by the aggregate, and the percent of the binder required to fill all but 4 percent of the voids in mineral aggregate. The percent of binder absorbed, P_{ba} , is calculated by:

$$P_{ba} = [100\ G_b]\ \frac{G_{se} - G_{agg}}{G_{agg}\ G_{se}} \tag{5-8}$$

The percent of the void space, excluding the aggregate pore volume, the binder needs to fill is calculated by:

$$P_{film} = VMA - 4 \tag{5-9}$$

Where the constant, 4, in the equation represents a design air void content for the compacted mixture of 4 percent. The total mass of binder, in g/cc, needed then is:

$$Wt_{AC} = [P_{ba} + P_{film}]\ G_b \tag{5-10}$$

The mass of the aggregate, in g/cc, in the mixture is:

$$Wt_{agg} = [100 - VMA - P_{ba}]\ G_{se} \tag{5-11}$$

The percent of binder by total mass of mixture is then:

$$\%AC = \frac{Wt_{AC}}{Wt_{agg} + Wt_{AC}} \tag{5-12}$$

The results of these calculations are shown in Table 5-4. These calculated values are within 0.1 to 0.3 percent binder as determined from the full mix design. Based upon these results, this method can be used to estimate the optimum binder content for large stone mixtures.

The suitability of several gradations can also be assessed by examining the VMA for each set of three compacted specimens. The LSAM-4 gradation has VMA around 14 percent while

the LSAM-2 VMA is about 12. Comparing these to the desired range of VMA presented in the Asphalt Institute's MS-2 (Figure 5-4), it can be seen that the VMA for the LSAM-2 are marginal while those for the LSAM-4 gradation are acceptable. This would indicate that the LSAM-4 gradation would be the better gradation.

Table 5-4. Calculated Asphalt Cement Content Using both Aggregate and Compacted Sample Properties

Properties	LSAM-2 (Coarsest)	LSAM-3	LSAM-4 (Finest)
Aggregate Properties			
Bulk Specific Gravity (BSG)	2.661	2.617	2.623
Mixture Properties			
Theoretical Maximum Specific Gravity	2.505	2.492	2.492
Bulk Specific Gravity, SSD	2.441	2.423	2.391
Effective Specific Gravity of Aggregate, G_{se}	2.678	2.662	2.663
VMA, %	12.22	12.44	13.9
Binder Absorbed by Aggregate, P_{ba}, %	0.25	0.21	0.10
Percent of Voids Needed for Binder Film, P_{film}, %	8.22	8.44	9.92
Mass of Asphalt Cement, Wt_{AC}, g/cc	8.72	8.91	10.32
Mass of Aggregate, Wt_{agg}, g/cc	234.4	2325	229.0
Percent AC (total weight of mix)	3.6	3.7	4.3
Percent AC Determined in Marshall Mix Design (total weight of mix)	3.3	3.8	4.3

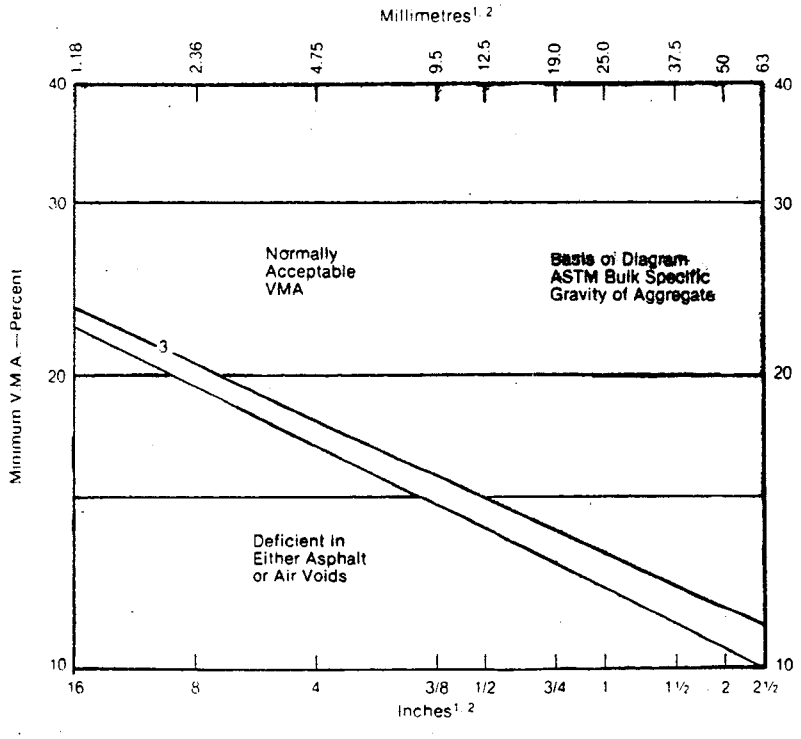

Figure 5-4. Acceptable VMA Values (19)

CHAPTER SIX

ANALYSIS

Temperature Susceptibility

The first comparison made was to determine the impact of increasing the sample diameter on the indirect tension test results. Table 6-1 compares resilient moduli values over a range of temperatures for the 100 and 150 mm (4 and 6 in) samples. This table shows that there was a tendency for the larger diameter samples to exhibit stiffer behavior. This difference was most likely the result of the differences in air voids between the two sets of samples. In general, as the air voids decreased, the mixture becomes stiffer.

Table 6-1. Comparison of Resilient Moduli for Two Specimen Diameters

Sample Diameter	Resilient Modulus at Various Temperatures, MPa (ksi)			Average Air Voids, %
	1°C (34°F)	25°C (77°F)	40°C (104°F)	
100 mm (4 in)	5,420 (786)	2,140 (301)	1,355 (194)	6.5
150 mm (6 in)	6350 (921)	3730 (541)	538 (78)	3.50

Figures 6-1 and 6-2 present a comparison of the resilient moduli over a range of test temperatures and frequencies for all 150 mm (6 in) diameter samples. The most obvious conclusion from this information is that LSAM gradations have a significantly reduced temperature susceptibility compared to the control mixture.

Figures 6-3 through 6-5 compare the moduli for the various test frequencies. Figure 6-3 shows that there was some dependence of the resilient moduli values on test frequency for the

control samples only at the coldest temperature. The LSAM gradations however exhibited frequency dependent moduli up to 25°C (77°F) (Figures 6-4, 6-5).

This frequency dependency at cold temperatures could be a function of several things. First, there is possibly a greater possibility of a viscous contribution from the binder due to the greater film thicknesses typical of LSAM gradations. Also, it was difficult to obtain sufficiently large strains (i.e., > 0.000125 mm) in the large samples at the cold temperatures; this could lead to thermal or electrical noise being read as actual material strains. Before a conclusion of frequency dependency of LSAM gradations at cold temperatures can be made, further, more in-depth, research is needed.

Previous research with the control mixture prepared in 100 mm (4 in) samples did not indicate a frequency dependency. Therefore, it is possible that the greater influence of the viscous response is partially a function of the sample geometry. The continued frequency dependency of the LSAM gradations could also be a function of the increased film thickness typical of these mixtures.

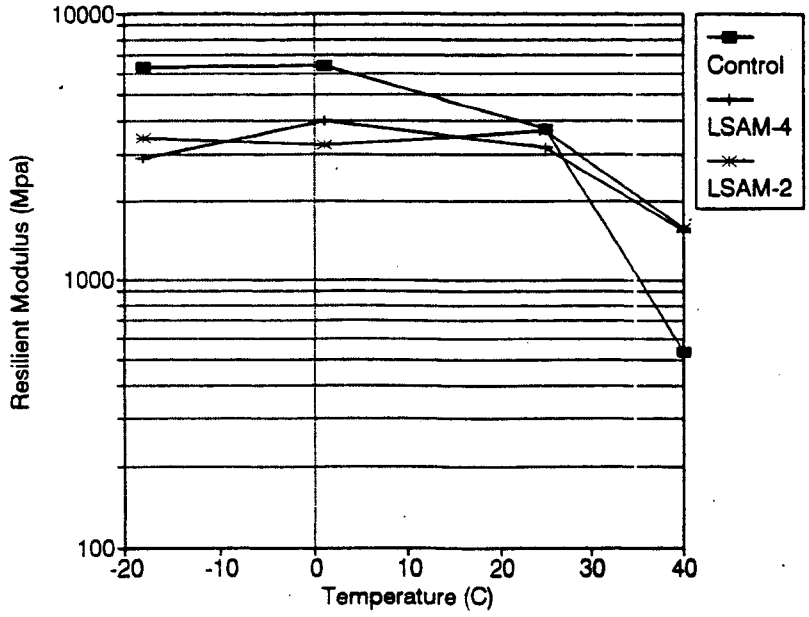

Figure 6-1. Temperature Susceptibility of Control and LSAM Samples (0.1 Sec. Load, 0.33 Hz.)

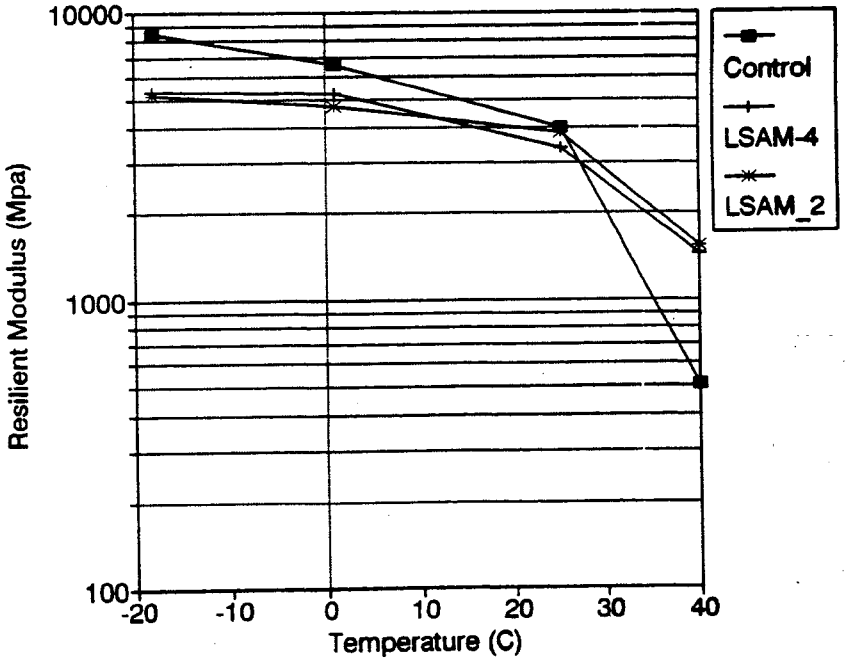

Figure 6-2. Temperature Susceptibility of Control and LSAM Samples (0.1 Sec. Load, 1 Hz.)

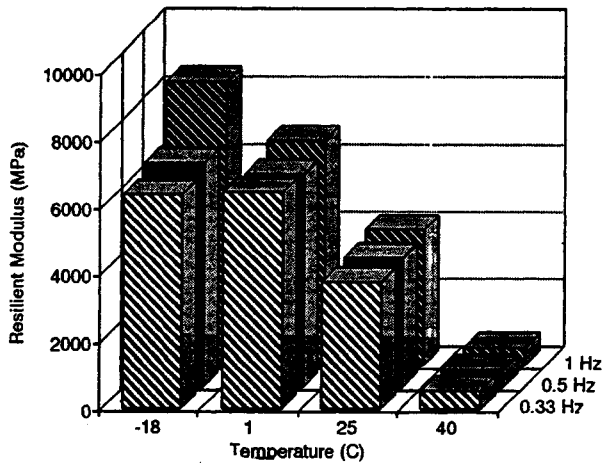

Figure 6-3. Influence of Test Frequency on Resilient Modulus (Control)

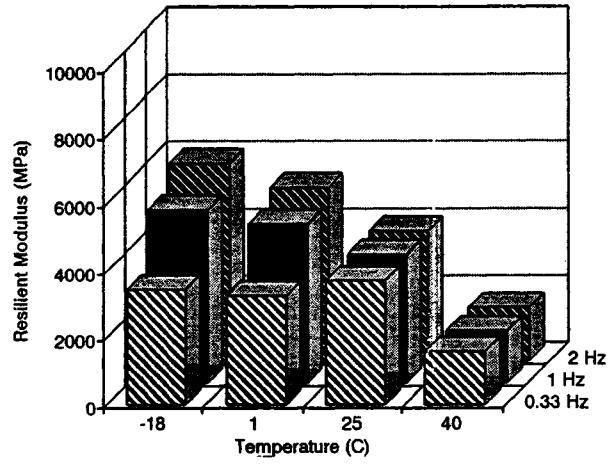

Figure 6-4. Influence of Test Frequency on Resilient Modulus (LSAM-2)

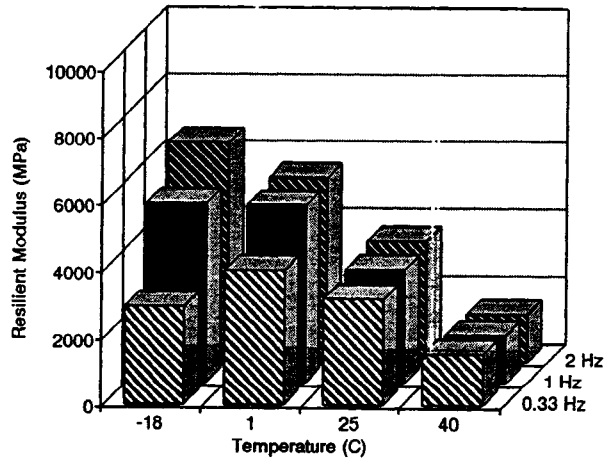

Figure 6-5. Influence of Test Frequency on Resilient Modulus (LSAM-4)

Moisture Sensitivity

Table 6-2 and Figures 6-6 through 6-8 present the results from the moisture sensitivity analysis. This information shows that as the gradation becomes coarser, the moisture sensitivity of the mixture increases. While the voids of both LSAM mixtures are similar, it is assumed that structure of the voids in the coarser LSAM-2 mixture are comprised of fewer but larger voids. This type of void structure would be more accessible to water intrusion. This hypothesis is supported by the levels of saturation seen in the coarser mixture. For the same level of saturation vacuum, 100 percent saturation was achieved for the LSAM-2 mixture while only 78 percent was obtained for the denser LSAM-4 mixture. The binder content is approximately the same for the control and the LSAM-4 gradation (4.3 and 4.7 percent binder, respectively); the binder content is about one percent lower for the LSAM-2 gradation (3.3 percent). This reduction in binder content might reflect a thinner protective film thickness on the aggregates.

The resilient modulus ratios decrease from 95 to 85 and 67 percent for the control, LSAM-4, and LSAM-2 gradations, respectively (Table 6-2, Figure 6-6). A similar trend is seen the tensile strength ratios (Table 6-2, Figure 6-6). Looking at the absolute values for resilient modulus after conditioning (Table 6-2, Figure 6-7), the LSAM-2 gradation still has a greater moduli than the control, even though this mixture shows only a 67 percent retained moduli. This is not the case for tensile strengths. The tensile strengths, even before conditioning, are significantly lower than the control mixture (Figure 6-8). This decrease in tensile strengths is enhanced by moisture conditioning.

While the binder content of the LSAM-4 is similar to that of the control, it is assumed that the binder in the LSAM mixture provides a thicker film thickness with reduced regions of

binder continuity within a given cross section; this cross section will also have larger, less well distributed voids. These factors are assumed to be responsible for the loss of tensile strength for the LSAM gradations since any mixture is dependent solely upon the binder matrix to develop a tensile strength.

Table 6-2. Moisture Sensitivity Test Results (0.1 Sec. Load, 0.33 Hz)

Sample	Resilient Modulus at 25 °C (77°F) MPa (ksi)			Tensile Strength at 25°C (77°F) kPa (psi)			Saturation Level %	Air Voids %
	Dry	Wet	Ratio	Dry	Wet	Ratio		
Control	2317 (336)	2200 (319)	95	1379 (200)	1372 (199)	100	84	2.50
LSAM-4	3303 (479)	2792 (405)	85	896 (130)	807 (117)	90	78	4.23
LSAM-2	3861 (560)	2586 (375)	67	986 (143)	607 (88)	62	100	4.39

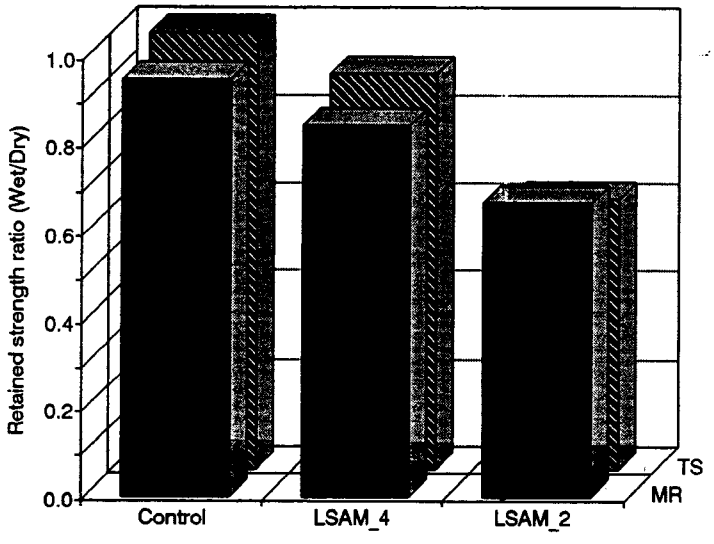

Figure 6-6. Retained Strength Ratios After Freeze/Thaw Conditioning for All Mixtures

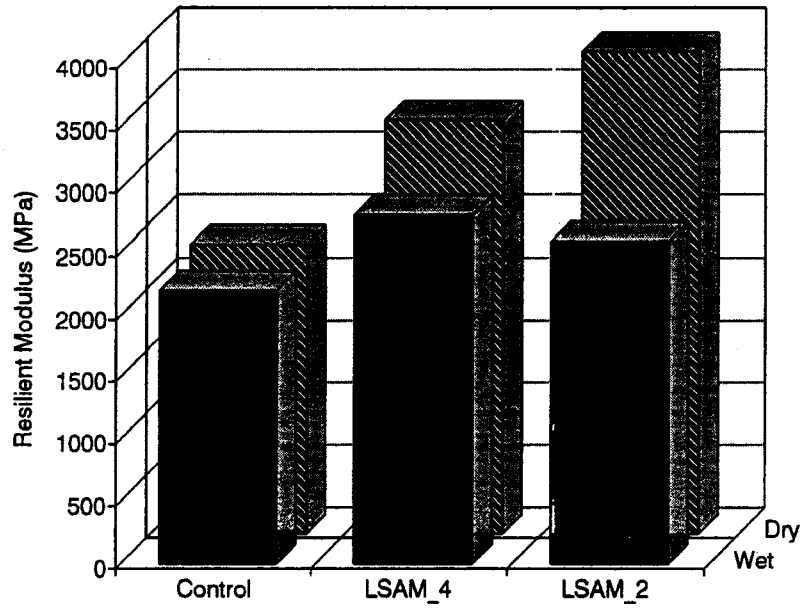

Figure 6-7. Resilient Modulus Values Before and After Conditioning for All Mixtures

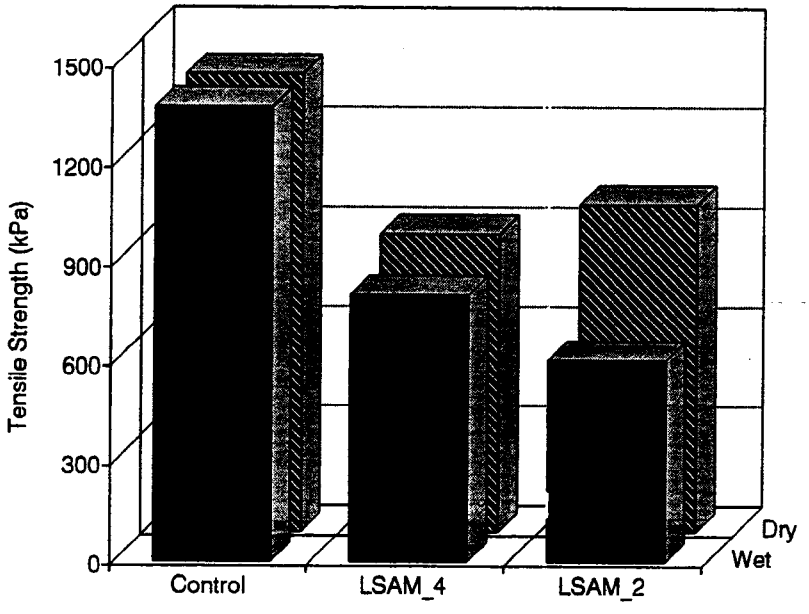

Figure 6-8. Tensile Strength Values Before and After Conditioning for All Mixtures

Low Temperature Behavior

Table 6-3 presents the maximum tensile strength and the corresponding total horizontal strain for -18 and 1°C (0 and 34°F) at a constant loading rate of 0.0025 mm/min (0.001 in/min). Figure 6-9 shows that the tensile strength decreases with increasing coarseness. However, a decrease in tensile strengths at cold temperatures usually indicates an increase in the ability of the material to strain. This ability to strain prevents a stress build-up and can be used as an indication of improved resistance to thermal cracking. Figure 6-10 shows that this is the case with these mixtures to some extent. Both of the LSAM gradations provided more ability to strain, or deform, prior to failure. The LSAM-2 and -4 gradations increased the ability of the mixture to strain over the control by approximately 72 and 300 percent, respectively, for either test temperature. This indicates that large stone mixtures can increase the resistance to thermal cracking but that there is an optimum gradation to achieve the best combination of results. In this case, the LSAM-4 gradation appears to be the best gradation.

Table 6-3. Low Temperature Behavior Under a Constant Strain Rate of 0.0025 mm/min (0.001 in/min)

Sample	-18°C (0°F)		1°C (34°F)	
	Maximum Tensile Strength kPa (psi)	Corresponding Total Horizontal Strain (μ-strain)	Maximum Tensile Strength kPa (psi)	Corresponding Total Horizontal Strain (μ-strain)
Control	5861 (850)	332	2041 (296)	1,581
LSAM-2	3206 (465)	579	889 (129)	2,663
LSAM-4	3972 (576)	903	1145 (166)	4,938

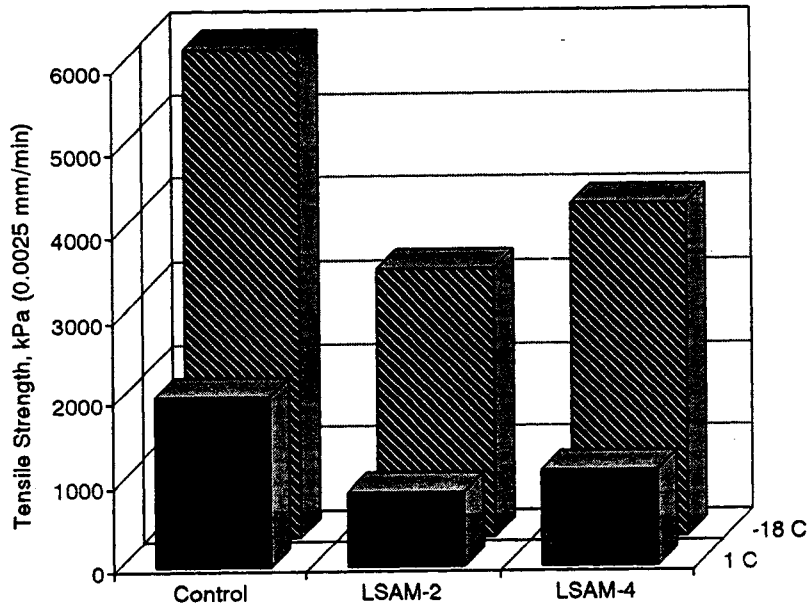

Figure 6-9. Maximum Tensile Strength at Cold Temperatures

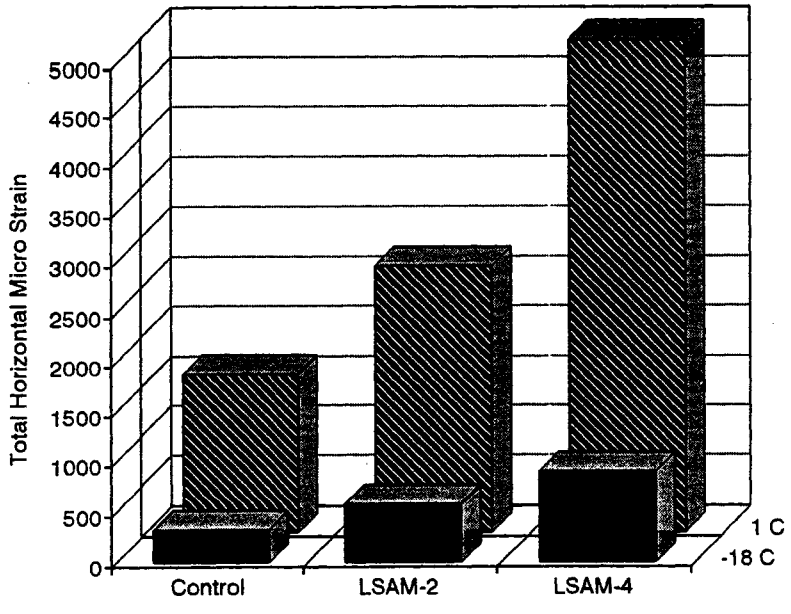

Figure 6-10. Total Horizontal Strain at Cold Temperatures

Permanent Deformation

Figures 6-11 and 6-12 show typical creep test results under different deviator stresses. Table 6-4 presents the Burgers model parameters calculated from Figures 6-11 and 6-12. As the deviator stress increased from 103 kPa (15 Psi) 310 kPa (45 psi), the material properties (E and η) of the control mixture were unaffected, but the LSAM mixes yielded. These results contradict the information obtained from the literature about field performance, which indicate that increasing the coarse aggregate proportion will increase the creep resistance of the mixture.

Table 6-5 presents the creep modulus at 30 minutes after the static test load was applied. This time was selected for comparing the tests as most of the samples survived the testing sequence up until this time. These data indicate an opposite trend as to what was expected. That is, the control mixtures performed better than the LSAM gradations. For the control mixture, as the deviator stress increased from 103 kPa (15 psi) to 310 kPa (45 psi), the creep modulus remained the same. However, for the LSAM mixes, as the deviator stress increased from 103 kPa (15 psi) to 310 kPa (45 psi), the creep moduli decreased and were similar for both LSAM gradations.

This apparent contradiction can most likely be explained by the difficulties encountered in preparing these very large samples. While the stacked samples for the control mixture appeared to work well, using the same approach with the LSAM gradations was difficult at best. When the tack coat was applied between each sample interface during sample fabrication, most of the tack coat filled the surface voids in the samples. This led to excessive amounts of tack coat being used to secure the individual lifts. This procedure also led to the formation of a weak interface as there were limited contact points between the lifts.

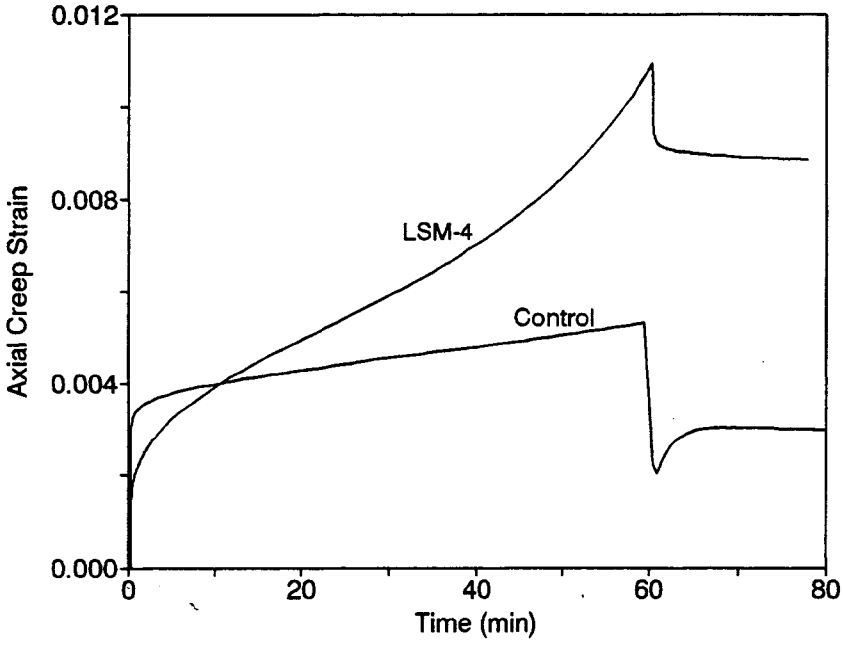

Figure 6-11. Typical Creep Test Result at 60°C (140°F) Deviator Stress 310 kPa (45 psi)

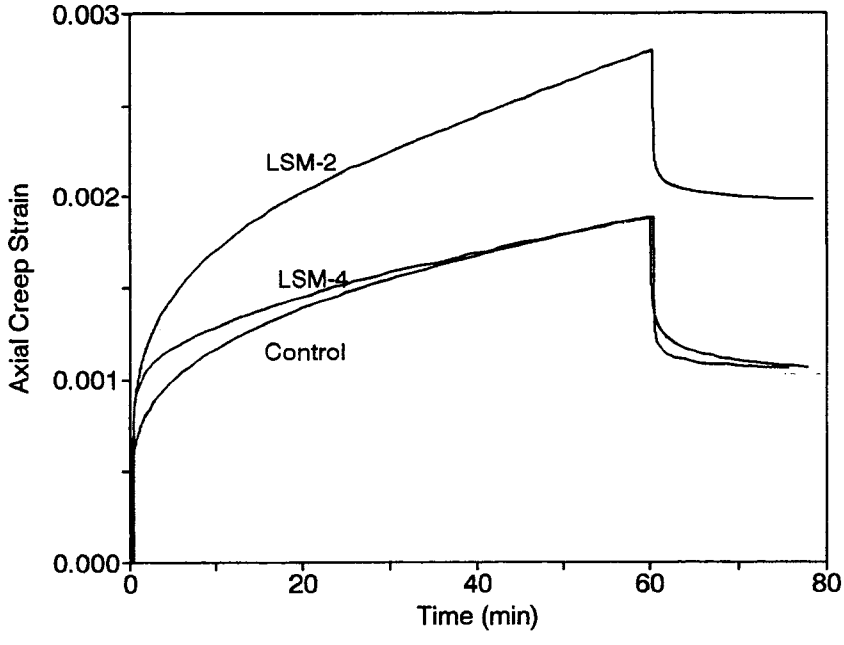

Figure 6-12. Typical Creep Test Result at 60°C (140°F) Deviator Stress 103 kPa (15 psi)

Table 6-4. Burger's Model Parameters

Burger's Parameters	Deviator Stress 45 psi			Deviator Stress 15 psi		
	LSAM-C	LSAM-2	LSAM-4	LSAM-C	LSAM-2	LSAM-4
E_1 kPa (psi)	241,900 (35,000)	N/A	241,900 (35,000)	207, 300 (30,000)	207,300 (30,000)	207,300 (30,000)
η_1 kPa min (psi min)	172,800 (25,000)	N/A	172,800 (25,000)	414,600 (60,000)	414,600 (60,000)	345,600 (50,000)
E_2/η_2 (1/min)	1.4	N/A	1.4	0.5	0.5	0.6
E_2 kPa (psi)	345,600 (50,000)	N/A	345,600 (50,000)	345,600 (50,000)	172,800 (25,000)	172,800 (25,000)
η_2 kPa min (psi min)	8,984,440 (1,300,000)	N/A	2,073,330 (300,000)	8,293,330 (1,200,000)	4,837,770 (700,000)	6,911,111 (1,000,000)

Table 6-5. Creep Modulus Results at 60°C (140°F)

Sample	Creep Modulus MPa (ksi)	
	Deviator stress 104 kPa (15 psi)	Deviator stress 310 kPa (45 psi)
Control	58.9 (8.5)	N/A
LSAM-2	69.3 (10.0)	48.5 (7)
LSAM-4	90.1 (13.0)	93.6 (13.5)

Based on these results, no conclusions can be drawn about the permanent deformation characteristics of the LSAM mixtures. If further work is to be done in this area, a rigorous development of preparation of these large samples needs to be completed before further testing is attempted.

CHAPTER SEVEN

CONCLUSIONS AND RECOMMENDATIONS

Conclusions

The following conclusions can be drawn from the information presented in this report:

1. A modified Marshall mix design can be used to determine the optimum binder content for large stone mixtures. Or, as an alternative, a combination of the preparation of one set of three samples and a volumetric calculation can be used to estimate the optimum binder content. This latter approach can significantly reduce material processing, sample preparation, and testing time as well as prevent excessive equipment wear and tear.
2. The determination of resilient modulus for the larger diameter samples (150 mm (6 inch)) tends to be dependent upon the test frequency. For conventional dense graded mixture, this frequency dependency only occurs at the colder (-18°C (0°F)) temperature. For the large stone mixtures, the moduli appear to be frequency dependent below 25°C (77°F). This behavior appears to be a function of both the specimen size as well as the increased binder film thickness for the large stone mixtures.
3. For mixtures with approximately similar air voids, the moisture sensitivity increases as the coarseness of the plus 4.75 mm (No. 4) increases.
4. The use of large stone mixtures can be expected to increase the mixture's resistance to thermal cracking. The resistance can be optimized by the selection of the gradation.
5. No conclusions could be reached for the permanent deformation testing other than the

samples are exceeding difficult to prepare. An improved method of preparing these samples needs to be developed before the permanent deformation characteristics of large stone mixtures can be evaluated.

Recommendations

The following recommendations are made with respect to the implementation of large stone asphalt mixture technology in Minnesota as well as future research needs.

1. A permissive specification for large-stone mixtures should be developed based upon LSAM-4 gradation used in this research project. This was the densest of the four LSAM gradations in this project. It was found to have the best overall properties of the large-stone mixtures studied, and it proved to be superior to the control gradation in many respects.
2. The method of volumetric mix design based upon aggregate and compacted sample properties (pp. 37 - 42) should be used when proportioning large-stone mixtures. Referring to the results of Table 5-4, it can be seen that very good agreement can be obtained between this method and the full Marshall mix design procedure. This approach requires less effort than the conventional Marshall approach; however, it does require the purchase and installation of the compaction equipment for large-diameter specimens.
3. As with any paving material, the use of LSAM should be based upon life-cycle economics. It would probably be best to consider its use in base and binder courses, especially in areas subjected to heavy truck loads where rutting in the asphalt mixture

may be anticipated. It may also be economical to use LSAM on low-volume roads when aggregate processing costs are higher for conventional mixtures with a smaller top-size aggregate.

4. Based upon the creep testing results presented herein, it would be wise to continue to investigate laboratory methods for permanent deformation testing of LSAM. Numerous problems with sample preparation and test procedures were noted during this project. This is necessary in order to develop a rational explanation of the behavior of permanent deformation of asphalt mixtures, and to develop better predictive procedures for field performance.

REFERENCES

1. Anderson, R.M., Epley, L.E. and Walker, D. "Kentucky's Experience with Large Size Aggregate and Bituminous Hot Mix," Journal of Asphalt Technology, Association of Asphalt Paving Technologists, Vol. 60, 1991.

2. Davis, R.L., Large Stone Mixes: A Historical Insight, National Asphalt Pavement Association, 1989.

3. Acott, M., "Today's Traffic Calls for Heavy Duty Asphalt Mixes," Roads and Bridges, Vol. 26, No. 1, Jan., 1988, pp. 39 - 45.

4. Marks, V.J., Monroe, R.W., and Adam, J.F., "Effect of Crushed Particles in Asphalt Mixtures," Transportation Research Record, No. 1259, Transportation Research Board, 1990, pp. 41 - 44.

5. Brown, E.R., and Bassett, C.E., "Effects of Maximum Aggregate Size on Rutting Potential and Other Properties of Asphalt - Aggregate Mixtures," Transportation Research Record, No. 1259, Transportation Research Board, 1990, pp. 107 - 119.

6. Button, J.W., Perdomo, D., and Lytton, R.L., "Influence of Aggregate on Rutting in Asphalt Concrete Pavements," Transportation Research Record, No. 1259, Transportation Research Board, 1990, pp. 141 - 152.

7. Kandhal, P.S., Testing and Evaluation of Large-Stone Mixes using Marshall Mix Design Procedures, Report, National Center for Asphalt Technology, Auburn University, 1990.

8. Kandhal, P.S., "Design of Large-Stone Mixes to Minimize Rutting," Transportation Research Record, No. 1259, Transportation Research Board, 1990, pp. 153 - 162.

9. Acott, M., The Design of Hot Mix Asphalt for Heavy Duty Pavements, National Asphalt Pavement Association, 1990.

10. Mahboub, K., and Allen, D.L., "Characterization of Rutting Potential of Large-Stone Asphalt Mixes in Kentucky," Transportation Research Record, No. 1259, Transportation Research Board, 1990, pp. 133 - 140.

11. Mahboub, K., and Williams, E.G., "Construction of Large-Stone Asphalt Mixes (LSAMs) in Kentucky," Transportation Research Record, No. 1282, Transportation Research Board, 1990, pp. 41 - 44.

12. ---, "Report on the 1990 European Asphalt Study Tour," American Association of State Highway and Transportation Officials, 1991.

13. Peter, A.F., "Use of Stone Mastic Asphalt in Germany, State-of-the-Art," paper submitted to the 71st Transportation Research Board meeting, 1992.

14. ---, "SHRP Product Catalog," Strategic Highway Research Program, 1992.

15. ---, "ASTM D1559 - 89, Test Method for Resistance to Plastic Flow of Bituminous Mixtures Using Marshall Apparatus," 1993 Annual Book of ASTM Standards, Vol. 4.03, American Society for Testing and Materials, 1993.

16. ---, "ASTM D4123 - 82 (1987), Test for Indirect Tension Test for Resilient Modulus Test of Bituminous Mixtures," 1993 Annual Book of ASTM Standards, Vol. 4.03, American Society for Testing and Materials, 1993.

17. ---" ASTM D4867 - 88, Test Method for Effect of Moisture on Asphalt Concrete Paving Mixtures," 1993 Annual Book of ASTM Standards, Vol. 4.03, American Society for Testing and Materials, 1993.

18. Roberts, F.L., Kandhal, P.S., Brown, E.R., Lee., D., Kennedy, T.W., Hot Mix Asphalt Materials, Mixture, Design, and Construction, 1st ed., National Asphalt Pavement Association Education Foundation, 1991.

19. ---, Mix Design Methods for Asphalt Concrete and Other Hot-Mix Types, Manual Series No. 2, The Asphalt Institute, 1988, pg. 32.

20. Hondos, G., "The Evaluation of Poisson's Ratio and the Modulus of Materials of a Low Tensile Resistance by the Brazilian (indirect tensile) Test with Particular Reference to Concrete," Australian Journal of Applied Science, Vol. 10, No. 3, September 1959.

21. Lytton, R.L., and Roque, R., "SHRP A-005 Performance Models and Validation of Test Results," Quarterly Report, Strategic Highway Research Program, July 15, 1991.

22. Kim, J.R., Characteristics of Permanent Deformation in Asphalt Concrete, Master of Science thesis, University of Minnesota, 1992.

23. Goodman, R.E., Introduction of Rock Mechanics, John Wiley & Sons, 1988.

APPENDIX A

THEORETICAL DISCUSSION OF DIAMETRAL TENSION AND UNIAXIAL COMPRESSION

Theory of Diametral Tension Test

Most research samples, except the creep samples, were tested using the indirect tension apparatus. The theory of indirect tension test done on a Marshall sample is based on elastic Theory. The stresses σ_{xx} and σ_{yy} along the X and Y axes for the loading configuration shown in Figure A-1 were derived by Hondros (20). According to Hondros' solution:

$$\sigma_{xx}(0,y) = \frac{2}{\pi}\frac{P}{at}\left[\frac{(1-\frac{y^2}{R^2})\sin 2\alpha}{(1-2\frac{y^2}{R^2}\cos 2\alpha+\frac{y^4}{R^4})} - \operatorname{atan}\left(\frac{1+\frac{y^2}{R^2}}{1-\frac{y^2}{R^2}}\tan\alpha\right)\right]$$

$$\sigma_{yy}(0,y) = -\frac{2}{\pi}\frac{P}{at}\left[\frac{(1-\frac{y^2}{R^2})\sin 2\alpha}{(1-2\frac{y^2}{R^2}\cos 2\alpha+\frac{y}{R^4})} + \operatorname{atan}\left(\frac{1+\frac{y^2}{R^2}}{1-\frac{y^2}{R^2}}\tan\alpha\right)\right]$$

$$\sigma_{xx}(x,0) = \frac{2}{\pi}\frac{P}{at}\left[\frac{(1-\frac{x^2}{R^2})\sin 2\alpha}{(1+2\frac{x^2}{R^2}\cos 2\alpha+\frac{x^4}{R^4})} - \operatorname{atan}\left(\frac{1-\frac{x^2}{R^2}}{1+\frac{x^2}{R^2}}\tan\alpha\right)\right] \qquad \text{(A-1)}$$

$$\sigma_{yy}(x,0) = -\frac{2}{\pi}\frac{P}{at}\left[\frac{(1-\frac{x^2}{R^2})\sin 2\alpha}{(1+2\frac{x^2}{R^2}\cos 2\alpha+\frac{x^4}{R^4})} + \operatorname{atan}\left(\frac{1-\frac{x^2}{R^2}}{1+\frac{x^2}{R^2}}\tan\alpha\right)\right]$$

Where:

P = Applied load, kN (psi)

a = Width of the loading strip, mm (in)

t = Thickness of the sample, mm (in)

R = Radius of the sample, mm (in)

2α = Angle as shown in Figure A-1, radians

Since $a = 2R \sin\alpha$, Equation(A-1) can be rewritten as:

$$\sigma_{xx}(0,y) = \frac{P}{\pi Rt}\frac{1}{\sin\alpha}\left[\frac{(1-\frac{y^2}{R^2})\sin 2\alpha}{(1-2\frac{y^2}{R^2}\cos 2\alpha+\frac{y^4}{R^4})} - \operatorname{atan}\left(\frac{1+\frac{y^2}{R^2}}{1-\frac{y^2}{R^2}}\tan\alpha\right)\right]$$

$$\sigma_{yy}(0,y) = -\frac{P}{\pi Rt}\frac{1}{\sin\alpha}\left[\frac{(1-\frac{y^2}{R^2})\sin 2\alpha}{(1-2\frac{y^2}{R^2}\cos 2\alpha+\frac{y^4}{R^4})} + \operatorname{atan}\left(\frac{1+\frac{y^2}{R^2}}{1-\frac{y^2}{R^2}}\tan\alpha\right)\right]$$

$$\sigma_{xx}(x,0) = \frac{P}{\pi Rt}\frac{1}{\sin\alpha}\left[\frac{(1-\frac{x^2}{R^2})\sin 2\alpha}{(1+2\frac{x^2}{R^2}\cos 2\alpha+\frac{x^4}{R^4})} - \operatorname{atan}\left(\frac{1-\frac{x^2}{R^2}}{1+\frac{x^2}{R^2}}\tan\alpha\right)\right] \qquad \text{(A-2)}$$

$$\sigma_{yy}(x,0) = -\frac{P}{\pi Rt}\frac{1}{\sin\alpha}\left[\frac{(1-\frac{x^2}{R^2})\sin 2\alpha}{(1+2\frac{x^2}{R^2}\cos 2\alpha+\frac{x^4}{R^4})} + \operatorname{atan}\left(\frac{1-\frac{x^2}{R^2}}{1+\frac{x^2}{R^2}}\tan\alpha\right)\right]$$

Define the dimensionless stress components as

$$\sigma' = \frac{\sigma}{\frac{P}{\pi R t}} \tag{A-3}$$

Equation (A-2) becomes

$$\sigma'_{xx}(0,y) = \frac{1}{\sin\alpha}\left[\frac{(1-\frac{y^2}{R^2})\sin 2\alpha}{(1-2\frac{y^2}{R^2}\cos 2\alpha+\frac{y^4}{R^4})} - \operatorname{atan}(\frac{1+\frac{y^2}{R^2}}{1-\frac{y^2}{R^2}}\tan\alpha)\right]$$

$$\sigma'_{yy}(0,y) = -\frac{1}{\sin\alpha}\left[\frac{(1-\frac{y^2}{R^2})\sin 2\alpha}{(1-2\frac{y^2}{R^2}\cos 2\alpha+\frac{y^4}{R^4})} + \operatorname{atan}(\frac{1+\frac{y^2}{R^2}}{1-\frac{y^2}{R^2}}\tan\alpha)\right]$$

$$\sigma'_{xx}(x,0) = \frac{1}{\sin\alpha}\left[\frac{(1-\frac{x^2}{R^2})\sin 2\alpha}{(1+2\frac{x^2}{R^2}\cos 2\alpha+\frac{x^4}{R^4})} - \operatorname{atan}(\frac{1-\frac{x^2}{R^2}}{1+\frac{x^2}{R^2}}\tan\alpha)\right] \tag{A-2a}$$

$$\sigma'_{yy}(x,0) = -\frac{1}{\sin\alpha}\left[\frac{(1-\frac{x^2}{R^2})\sin 2\alpha}{(1+2\frac{x^2}{R^2}\cos 2\alpha+\frac{x^4}{R^4})} + \operatorname{atan}(\frac{1-\frac{x^2}{R^2}}{1+\frac{x^2}{R^2}}\tan\alpha)\right]$$

Figures A-2 and A-3 show the corresponding stress distribution. At the center of the specimen, where $x = y = 0.0$, the stresses along the horizontal and vertical axes are:

$$\sigma'_{xx}(0,0) = \frac{\sin 2\alpha - \alpha}{\sin\alpha}$$

$$\sigma'_{yy}(0,0) = -\frac{\sin 2\alpha + \alpha}{\sin\alpha} \tag{A-4}$$

Both plane stress and plane strain loading conditions can be considered from this set of solution and some useful guidelines can be obtained from such analysis.

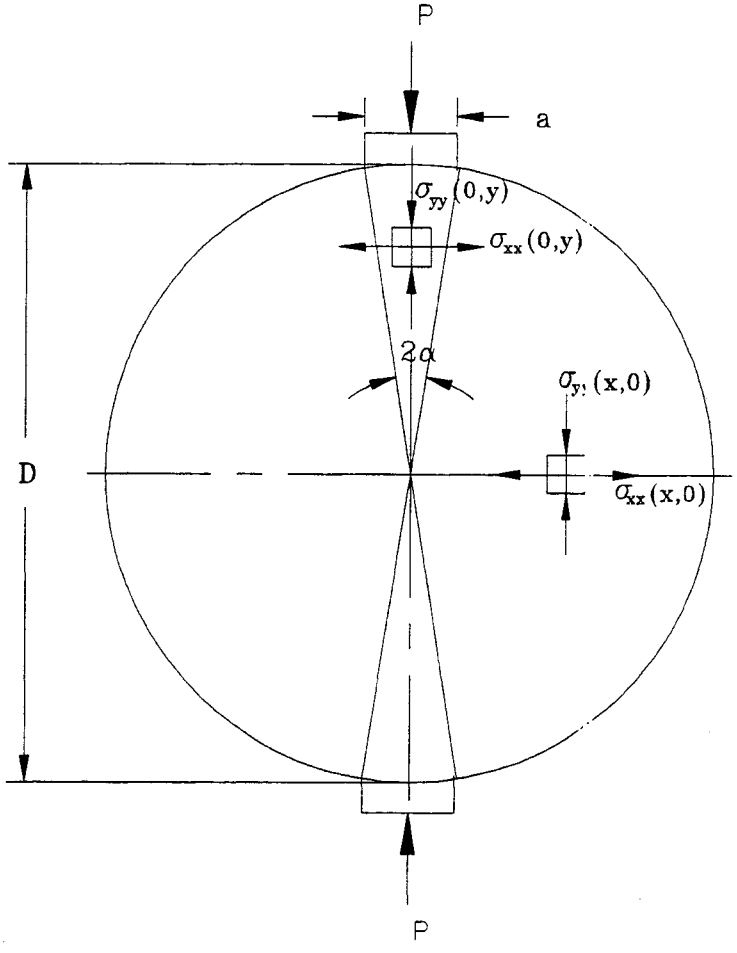

Figure A-1. Loading Configuration of Indirect Tension Test (20)

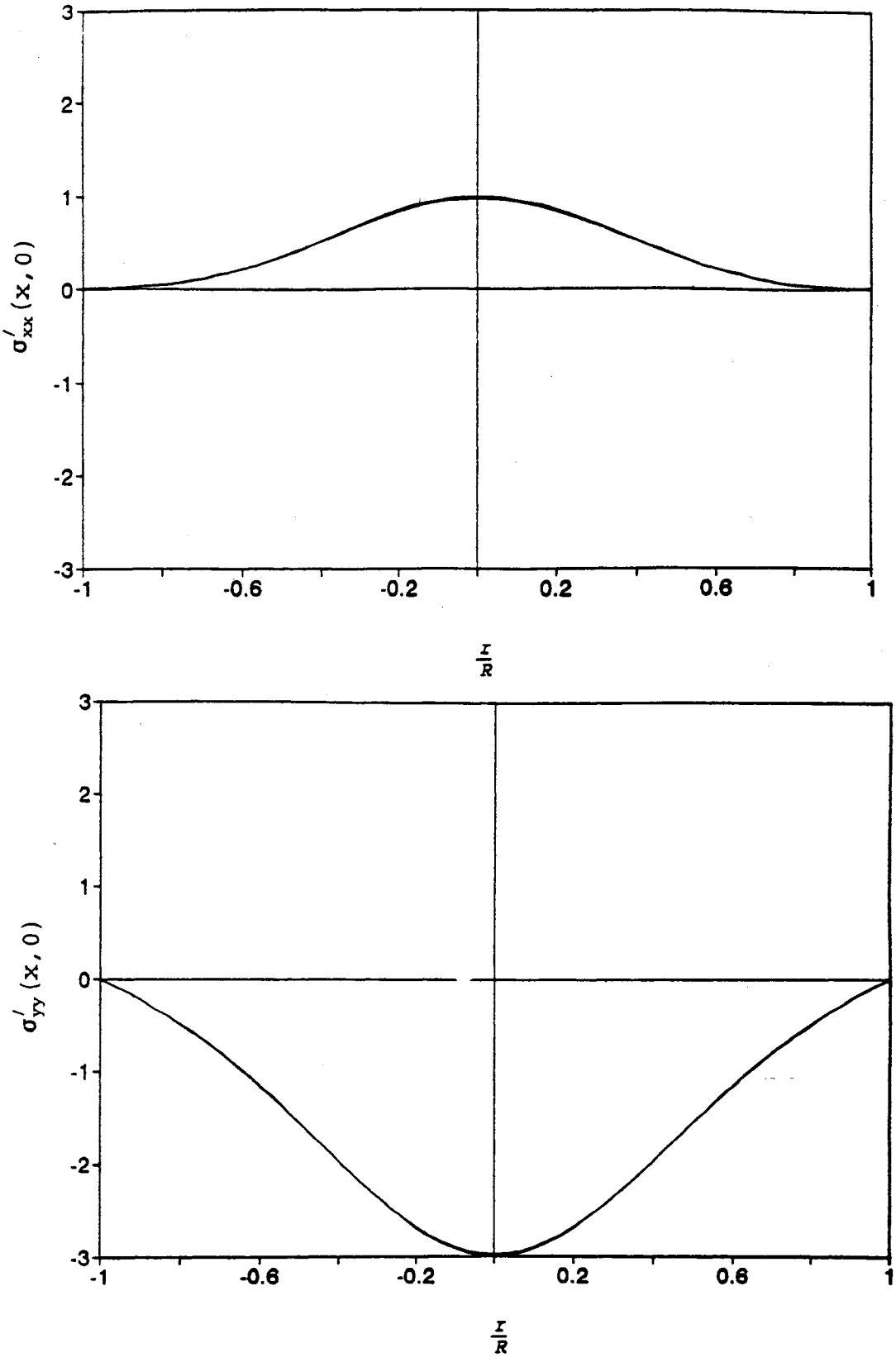

Figure A-2. Stress Distribution Along The Horizontal Axis

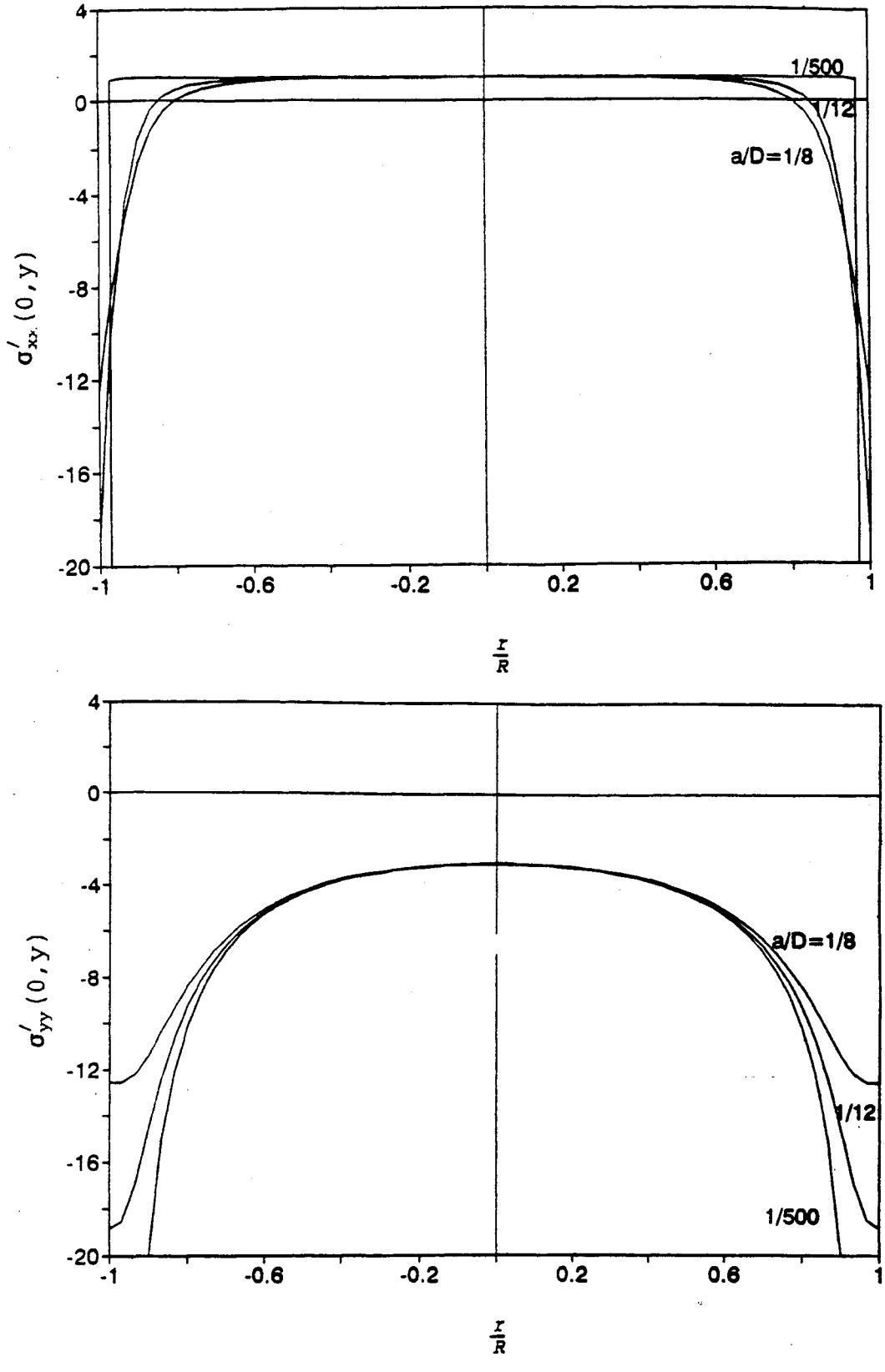

Figure A-3. Stress Distribution Along The Vertical Axis

Plane Stress Conditions

Assuming plane stress condition, let E be the Young's modulus and υ be the Poisson's ratio. According to Hooke's law:

$$\epsilon_{xx} = \frac{1}{E}[\sigma_{xx} - \upsilon\sigma_{yy}]$$
$$\epsilon_{yy} = \frac{1}{E}[\sigma_{yy} - \upsilon\sigma_{xx}] \qquad \text{(A-5)}$$

There are two ways to determine E and υ from a laboratory experiment. We can measure the strain components at any point inside the domain where the corresponding stress components can be calculated using equation (A-2a) and then solve for E and υ from equation (A-5). Or we can measure the total change in length across the X and Y axes which are the integration of (A-5) and than solve for E and υ. The latter is experimentally easier to achieve and the E and υ thus determined are average properties of a block of material. For asphalt concrete, the material properties are not uniform on a point to point basis due to the differences between the aggregate and mortar, but are uniform on a block to block basis. So the second approach is used for asphalt concrete. Let the total change in diameter across the horizontal axis is ΔU and the total change in diameter across the vertical axis is ΔV, then

$$\Delta U = \int_{-R}^{R} \epsilon_{xx}(x,0)dx = \frac{1}{E}\int_{-R}^{R}[\sigma_{xx}(x,0) - \upsilon\sigma_{yy}(x,0)]dx$$
$$\Delta V = \int_{-R}^{R} \epsilon_{yy}(0,y)dy = \frac{1}{E}\int_{-R}^{R}[\sigma_{yy}(0,y) - \upsilon\sigma_{xx}(0,y)]dy \qquad \text{(A-6)}$$

Define

$$I_1 = \int_{-R}^{R} \sigma_{xx}(0,y)dy \qquad I_2 = \int_{-R}^{R} \sigma_{yy}(0,y)dy$$
$$I_3 = \int_{-R}^{R} \sigma_{xx}(x,0)dx \qquad I_4 = \int_{-R}^{R} \sigma_{yy}(x,0)dx \tag{A-7}$$

The values of I_1 to I_4 are calculated using numerical integration and are listed in Table A-1.

Table A-1. Results of Numerical Integrations (times $2P/\pi t$).

Ratio of Loading Strip Width to Sample Diameter (a/D)	Integration Parameters			
	I_1	I_2	I_3	I_4
1/8	-0.09866	-5.63559	0.42395	-1.57078
1/12	-0.06566	-6.41790	0.42688	-1.57078
1/20	-0.03939	-7.41550	0.42837	-1.57078
1/100	-0.00797	-10.60415	0.42917	-1.57078
1/500	-0.00201	-13.81679	0.42920	-1.57078

Solving the equations in (A-6) for υ, we have

$$\upsilon = \frac{I_2\Delta U - I_3\Delta V}{I_1\Delta U - I_4\Delta V} = \frac{I_2 - I_3\frac{\Delta V}{\Delta U}}{I_1 - I_4\frac{\Delta V}{\Delta U}} \tag{A-8}$$

from (A-5)

$$E = \frac{1}{\Delta U}(I_3 - \upsilon I_4) \tag{A-9a}$$

or

$$E = \frac{1}{\Delta V}(I_2 - \upsilon I_1) \tag{A-9b}$$

and the tensile strain at the center of the specimen is

$$\epsilon_t(0,0)=\frac{1}{E}[\sigma_{xx}(0,0)-\upsilon\sigma_{yy}(0,0)] \qquad \text{(A-10)}$$

Substituting the values of I_1 to I_4 into equations (A-8), (A-9a), and (A-10), we can arrive at the expressions for E , υ and ϵ_t (0, 0). However, by observing Table A-1 one can notice that I_1 and I_2 vary with the a/D ratio, but I_3 and I_4 are virtually independent of the a/D ratio. So the expressions for E, υ, and ϵ_t (0, 0) will depend on a/D. In the current ASTM standard (ASTM D4123), equation (A-9a) is used for calculating the resilient modulus, and equation (A-10) is used for calculating the tensile strain. The dimensionless values of the stress components at the center of the specimen can be calculated according to equation (A-4) and the results are listed in Table A-2

Table A-2. Dimensionless Stress Values at the Center of the Specimen

a/D	σ'_{xx} (0,0)	σ'_{yy} (0,0)
1/8	0.98169	-2.98694
1/12	0.99188	-2.99420
1/20	0.99708	-2.99792
1/100	0.99988	-2.99992
1/500	0.99999	-3.00000

It can be seen that σ'_{xx} (0,0) and σ'_{yy} (0,0) do not depend on the a/D ratio. Substitute the values of I_3, I_4, σ'_{xx} (0,0), and σ'_{yy} (0,0) into equations (A-9a) and (A-10) result in

$$E = \frac{1}{\Delta U}\frac{P}{t}(0.2727+\upsilon) \qquad \text{(A-11a)}$$

$$\epsilon_t(0,0) = \frac{\Delta U}{D}\frac{0.99708+2.99792\upsilon}{0.42837+1.57078\upsilon} \qquad \text{(A-11b)}$$

The expression for υ as a function of a/D is summarized in Table A-3. The variation of υ as a function of a/D at different values of $\Delta V/\Delta U$ is plotted in Figure A-4. It has been reported that Poisson's ratio determined in this manner are usually unreasonable. The current practice is to assume a value of υ for each specimen, it is claimed that the resilient modulus E and the tensile strain ϵ_t (0, 0) are relatively insensitive to the variation of υ. Figures A-5 and A-6 show the variations of E and ϵ_t (0, 0) with respect to υ.

Assuming a material parameter before the test makes the test result more subjective and thus less reliable. This problem can be resolved by changing the integration range. The non-unique expression for υ is due to the fact that it involves the terms I_1 and I_2 which are very sensitive to the a/D ratio. From Figures A-2 and A-3 it can be seen that stresses along the horizontal axis do not depend on the a/D ratio, but stresses along the vertical axis do. This is why I_1 and I_2 vary with a/D, but I_3 and I_4 do not. However, stress deviations along the vertical axis happen only near the loaded boundary. Sufficiently far away from the loaded area, stress distributions along the vertical axis are independent of a/D. Therefore, instead of measuring the total change in diameter across the vertical diameter, the longitudinal deformation across the center part of the specimen can be measured where the stress distributions are independent of the a/D ratio. This way the stress concentration problem can be avoided and the stress integrations along the vertical axis are independent of a/D, thus arriving at an unique expression

for υ. The numerical integrations along the center part of the specimen are recalculated and listed in Table A-4.

Table A-3. Expression for Poisson's Ratio, $\upsilon = (I_2 - I_3 \beta) / (I_1 - I_4 \beta)$

a/D	υ
1/8	$\frac{-5.63559 - 0.42395\beta}{-0.09866 + 1.57078\beta}$
1/12	$\frac{-6.41819 - 0.42688\beta}{-0.06796 + 1.57078\beta}$
1/20	$\frac{-7.41550 - 0.42837\beta}{-0.03939 + 1.57078\beta}$
1/100	$\frac{-10.60415 - 0.42917\beta}{-0.00797 + 1.57078\beta}$
1/500	$\frac{-13.81679 - 0.42920\beta}{-0.00201 + 1.57078\beta}$

where $\beta = \Delta V / \Delta U$

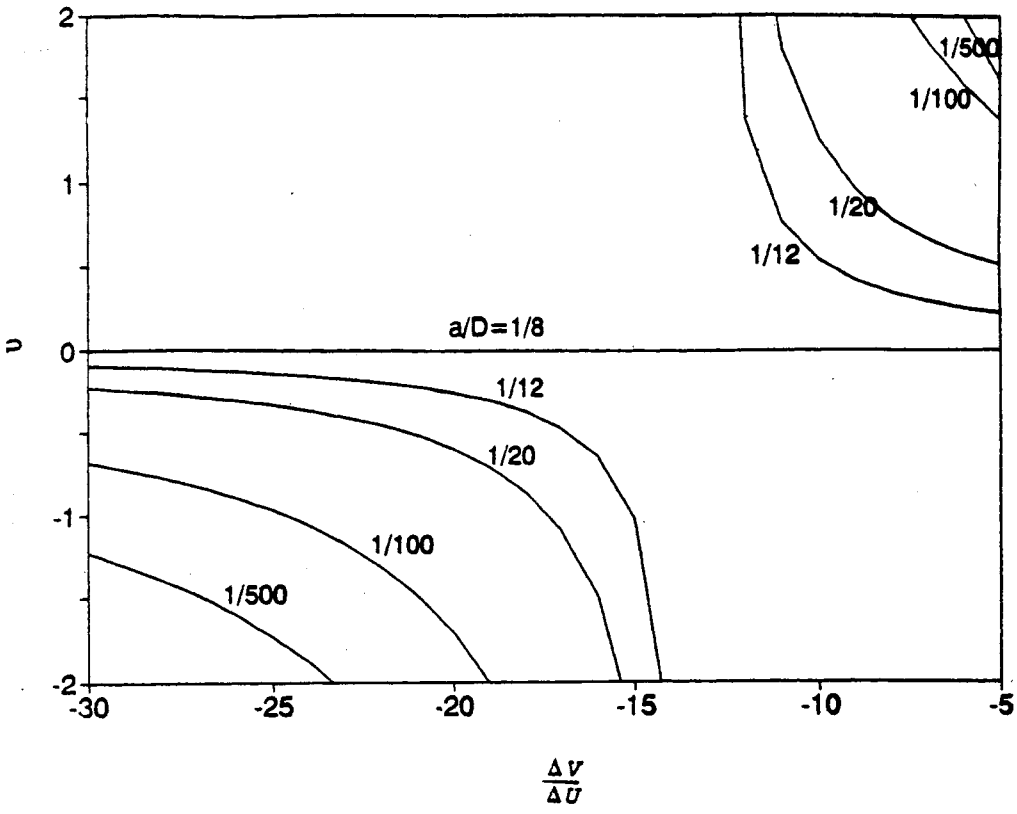

Figure A-4. Poisson's Ratio Versus ΔV/ΔU

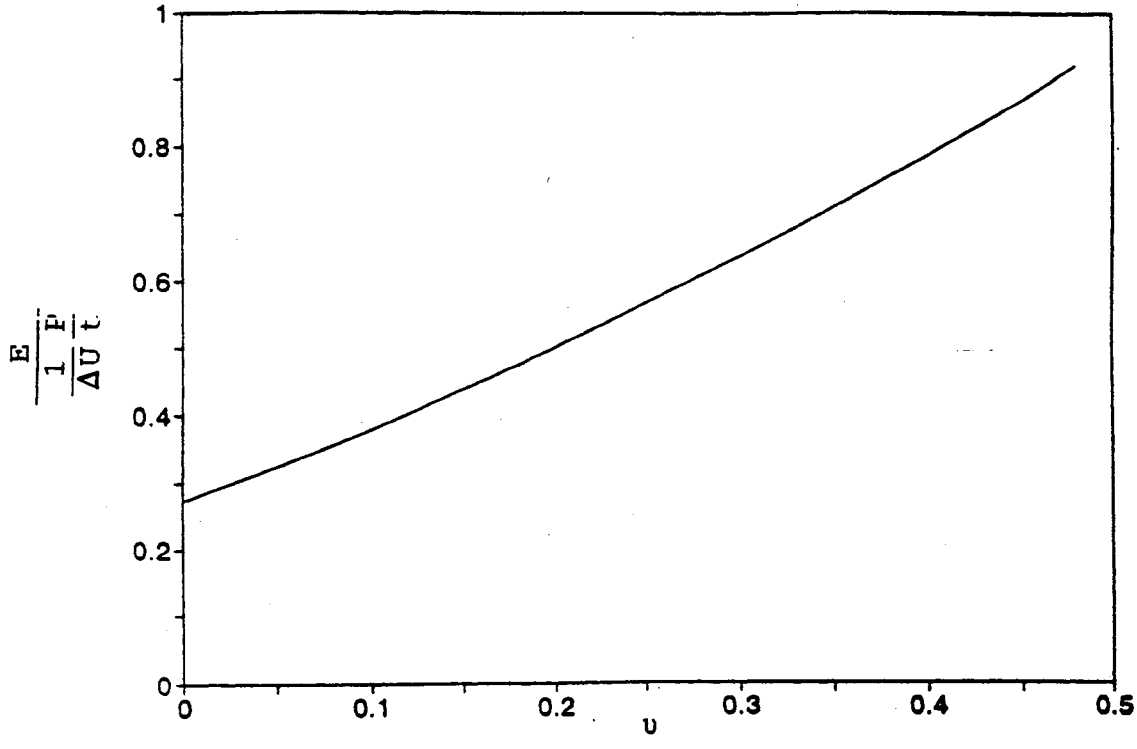

Figure A-5. Young's Modulus Versus Poisson's Ratio

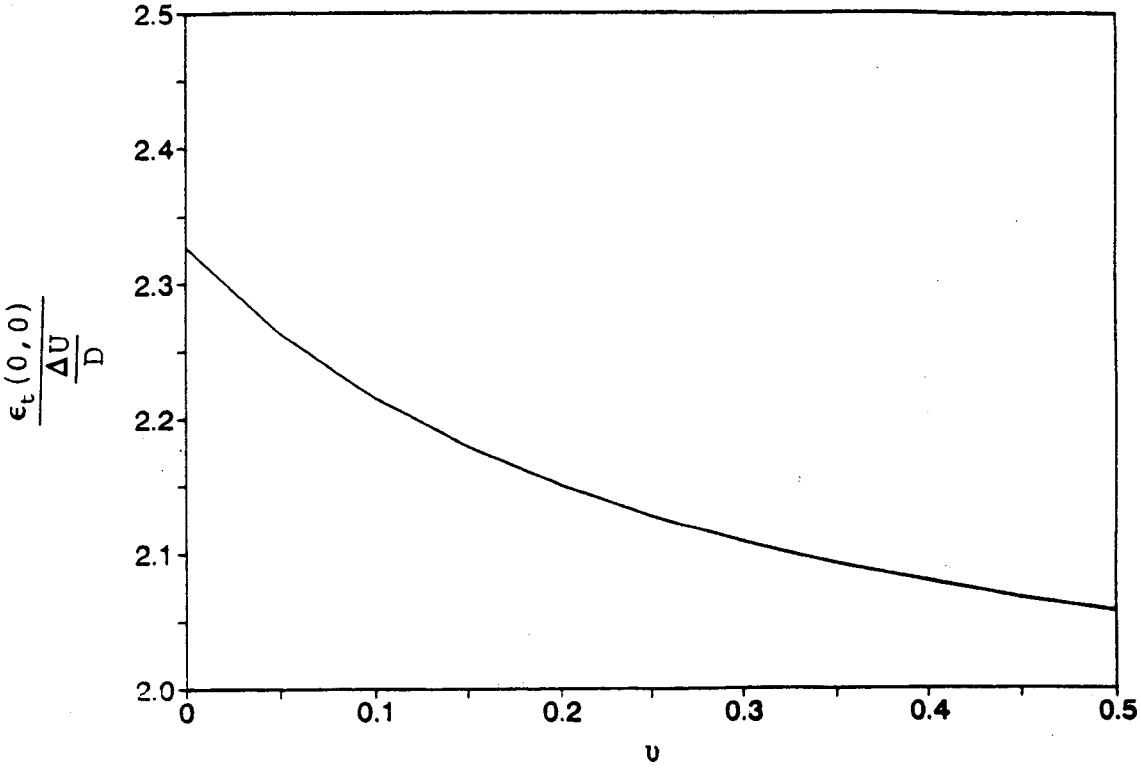

Figure A-6. Tensile Strain Versus Poisson's Ratio

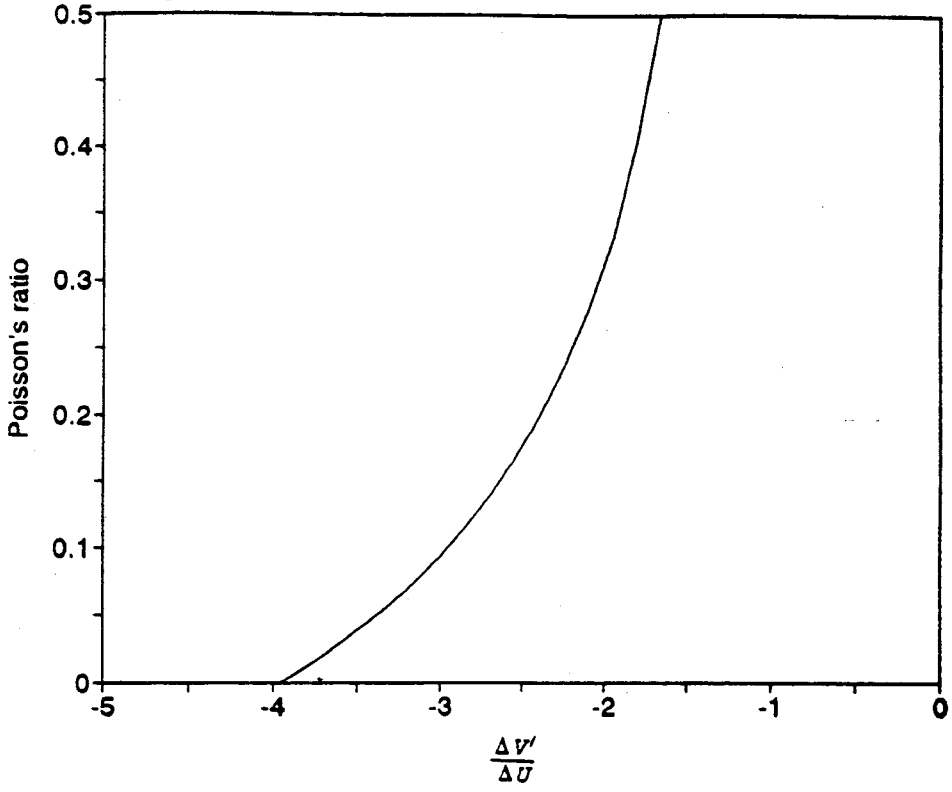

Figure A-7. Poisson's Ratio Versus ΔV'/ΔU

Table A-4. Numerical Integrals Along Part of the Axes

a/D	I_1 '	I_2 '	I_3 '	I_4 '
	r = 0.1 R			
1/8	0.098127	-0.29999	0.096896	-0.2961
1/12	0.099169	-0.30074	0.097887	-0.29679
1/20	0.099701	-0.30113	0.098382	-0.29715
1/100	0.099988	-0.30134	0.098665	-0.29734
1/500	0.1	-0.30135	0.098676	-0.29734
	r= 0.3R			
1/8	0.293224	-0.93253	0.26183	-0.83078
1/12	0.296991	-0.93563	0.265605	-0.83221
1/20	0.298917	-0.93721	0.266839	-0.83293
1/100	0.299957	-0.93807	0.267503	-0.83333
1/500	0.299998	-0.93810	0.26753	-0.83334
	r = 0.5R			
1/8	0.48293	-1.67996	0.367453	-1.22528
1/12	0.492377	-1.68954	0.370374	-1.22638
1/20	0.497249	-1.69449	0.371859	-1.22695
1/100	0.49989	-1.69717	0.372659	-1.22725
1/500	0.499996	-1.69728	0.372691	-1.22726
	r =0.7R			
1/8	0.648538	-2.70185	0.412839	-1.46023
1/12	0.676457	-2.73851	0.415794	-1.46067
1/20	0.691393	-2.7581	0.417297	-1.46089
1/100	0.699653	-2.76893	0.418105	-1.46102
1/500	0.699986	-2.76936	0.418137	-1.46102
	r = 0.9 R			
1/8	0.59306	-4.41132	0.423587	-1.56
1/12	0.726165	-4.67495	0.426518	-1.56005
1/20	0.826007	-4.85999	0.428008	-1.56007
1/100	0.896691	-4.98482	0.42881	-1.56008
1/500	0.899867	-4.99031	0.428842	-1.56009

where

$$I_1' = \int_{-r}^{r} \sigma_{xx}(0,y)dy \qquad I_2' = \int_{-r}^{r} \sigma_{yy}(0,y)dy$$
$$I_3' = \int_{-r}^{r} \sigma_{xx}(x,0)dx \qquad I_4' = \int_{-r}^{r} \sigma_{yy}(x,0)dx \tag{A-12}$$

It can be seen that within the range of [-0.5R, 0.5R], all the integrals are virtually independent of the a/D ratio. Let $\Delta V'$ be the total deformation along the vertical axis within the range of $-0.5R \leq y \leq 0.5R$, ΔU be the total deformation across the horizontal axis, then the expression for Poisson's ration becomes:

$$\upsilon = \frac{I_2' - I_3 \frac{\Delta V'}{\Delta U}}{I_1' - I_4 \frac{\Delta V'}{\Delta U}} = \frac{-1.69449 - 0.42837 \frac{\Delta V'}{\Delta U}}{0.49725 + 1.57078 \frac{\Delta V'}{\Delta U}} \tag{A-13}$$

The above expressions do not depend on the a/D ratio, and the relationship between Poisson's ratio and $\Delta V'/\Delta U$ is plotted in Figure A-7. It should be pointed out that we can also measure the longitudinal deformation at any other range within which stress distributions do not depend on the a/D ratio, it can be along either the horizontal or the vertical axis.

Plane Strain Conditions

Again, according to Hooke's law

$$\epsilon_{xx} = \frac{1}{E}[\sigma_{xx} - \upsilon(\sigma_{yy} + \sigma_{zz})]$$

$$\epsilon_{yy} = \frac{1}{E}[\sigma_{yy} - \upsilon(\sigma_{xx} + \sigma_{zz})] \qquad \text{(A-14)}$$

$$\epsilon_{zz} = \frac{1}{E}[\sigma_{zz} - \upsilon(\sigma_{xx} + \sigma_{yy})] = 0$$

eliminate σ_{zz} ,

$$\epsilon_{xx} = \frac{1}{E}[\sigma_{xx} - \upsilon\sigma_{yy} - \upsilon^2(\sigma_{xx} + \sigma_{yy})]$$

$$\epsilon_{yy} = \frac{1}{E}[\sigma_{yy} - \upsilon\sigma_{xx} - \upsilon^2(\sigma_{xx} + \sigma_{yy})] \qquad \text{(A-15)}$$

again by definition,

$$\Delta U = \int_{-R}^{R} \epsilon_{xx}(x,0)dx = \frac{1}{E}[I_3 - \upsilon I_4 - \upsilon^2(I_3 + I_4)]$$

$$\Delta V = \int_{-0.5R}^{0.5R} \epsilon_{yy}(0,y)dy = \frac{1}{E}[I_2' - \upsilon I_1' - \upsilon^2(I_1' + I_2')] \qquad \text{(A-16)}$$

from (A-16)

$$I_2' - \upsilon I_1' - \upsilon^2(I_1' + I_2') = [I_3 - \upsilon I_4 - \upsilon^2(I_3 + I_4)]\frac{\Delta V}{\Delta U} \qquad \text{(A-17)}$$

rearrange

$$[(I_3 + I_4)\frac{\Delta V}{\Delta U} - (I_1' + I_2')]\upsilon^2 + (I_4\frac{\Delta V}{\Delta U} - I_1')\upsilon + (I_2' - I_3\frac{\Delta V}{\Delta U}) = 0 \qquad \text{(A-18)}$$

define

$$a = (I_3+I_4)\frac{\Delta V}{\Delta U}-(I_1'+I_2')$$

$$b = (I_4\frac{\Delta V}{\Delta U}-I_1') \qquad \text{(A-19)}$$

$$c = (I_2'-I_3\frac{\Delta V}{\Delta U})$$

equation (A-18) becomes

$$a\upsilon^2 + b\upsilon + c = 0 \qquad \text{(A-20)}$$

solve for υ

$$\upsilon = \frac{-b\pm\sqrt{b^2-4ac}}{2a} \qquad \text{(A-21)}$$

If the values of I_1' , I_2' , I_3, and I_4 are substituted into (A-21) (remember $\Delta V / \Delta U < 0$), it can be shown that $a > 0$, $b < 0$, and $c < 0$. So for the Poisson's ratio to be meaningful, we should take the positive root.

$$\upsilon = \frac{-b+\sqrt{b^2-4ac}}{2a} \qquad \text{(A-22)}$$

from (A-16),

$$E = \frac{1}{\Delta U}\frac{2P}{\pi t}[I_3-\upsilon I_4-\upsilon^2(I_3+I_4)] \qquad \text{(A-23)}$$

In summary, for a plane stress condition:

$$\upsilon = \frac{I_2' - I_3\frac{\Delta V}{\Delta U}}{I_1' - I_4\frac{\Delta V}{\Delta U}}$$

$$E = \frac{1}{\Delta U}(I_3 - \upsilon I_4) \qquad \text{(A-24)}$$

$$\epsilon_t(0,0) = \frac{1}{E}[\sigma_{xx}(0,0) - \upsilon\sigma_{yy}(0,0)]$$

and for a plane strain condition:

$$\upsilon = \frac{-b+\sqrt{b^2-4ac}}{2a}$$

$$E = \frac{1}{\Delta U}[I_3 - \upsilon I_4 - \upsilon^2(I_3+I_4)] \qquad \text{(A-25)}$$

$$\epsilon_t(0,0) = \frac{1}{E}[\sigma_{xx}(0,0) - \upsilon\sigma_{yy}(0,0) - \upsilon^2(\sigma_{xx}(0,0)+\sigma_{yy}(0,0))]$$

where

$$\sigma_{xx}(0,0) = \frac{2P}{\pi Dt}$$

$$\sigma_{xx}(0,0) = 3\frac{2P}{\pi Dt} \qquad \text{(A-26)}$$

$$I_1' = 0.49725\frac{2P}{\pi t}$$

$$I_2' = -1.69449\frac{2P}{\pi t}$$

$$I_3 = 0.42837\frac{2P}{\pi t} \qquad \text{(A-27)}$$

$$I_4 = -1.57078\frac{2P}{\pi t}$$

$$a = (I_3+I_4)\frac{\Delta V}{\Delta U}-(I_1'+I_2')$$

$$b = (I_4\frac{\Delta V}{\Delta U}-I_1') \qquad \text{(A-28)}$$

$$c = (I_2'-I_3\frac{\Delta V}{\Delta U})$$

The υ - $\Delta V/\Delta U$ and E - $\Delta V/\Delta U$ relationships for both plane stress and plane strain conditions are plotted in Figures A-8 and A-9. It can be seen that the Poisson's ratios are virtually identical for plane stress and plane strain conditions. The difference in Young's moduli start to show up when $\Delta V / \Delta U > -2.5$.

The following conclusions can be drawn from this analysis:

1. Hondros' solution is suitable for diametral tension test.

2. Unified expressions for E, $\epsilon_t(0,0)$, and υ can be derived if properly selected measurements are obtained within a certain range along the horizontal or vertical axis.

3. The feasibility of designing a device that will allow the installation of either a strain gauge or a extensometer across the center part of the specimen to make the above measurement has been explored by researchers at Penn State University for the Strategic Highway Research Program (SHRP) (21). While there were some problems with matching signal conditioning with the sub-miniature LVDTs used, the last report from the researchers indicate these problems have been solved. Some form of this concept should be pursued in further research programs.

4. This proposed modification to the test method does not require an assumed value of υ. Poisson's ratio, resilient modulus, and tensile strain can all be determined experimentally. The accuracy of experiment can be greatly improved.

Due to time limitations for this program, equipment modifications were not possible. Therefore, the ASTM D4123 standard testing protocol (16) was used to determine the resilient modulus. The Poisson's ratio were assumed to be 0.2 for temperatures -18°C (0^0F) and 1°C (34 ^{0}F), 0.35 for 25°C (77 ^{0}F), and 0.5 for 40°C (104°F).

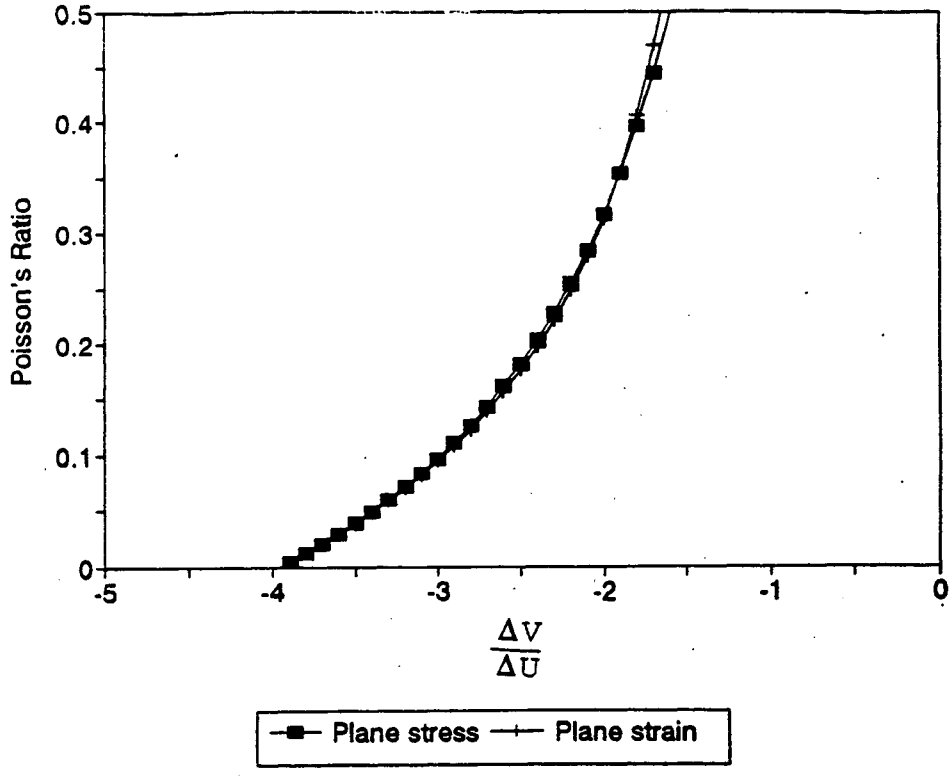

Figure A-8. Poisson's Ratio Versus ΔV/ΔU

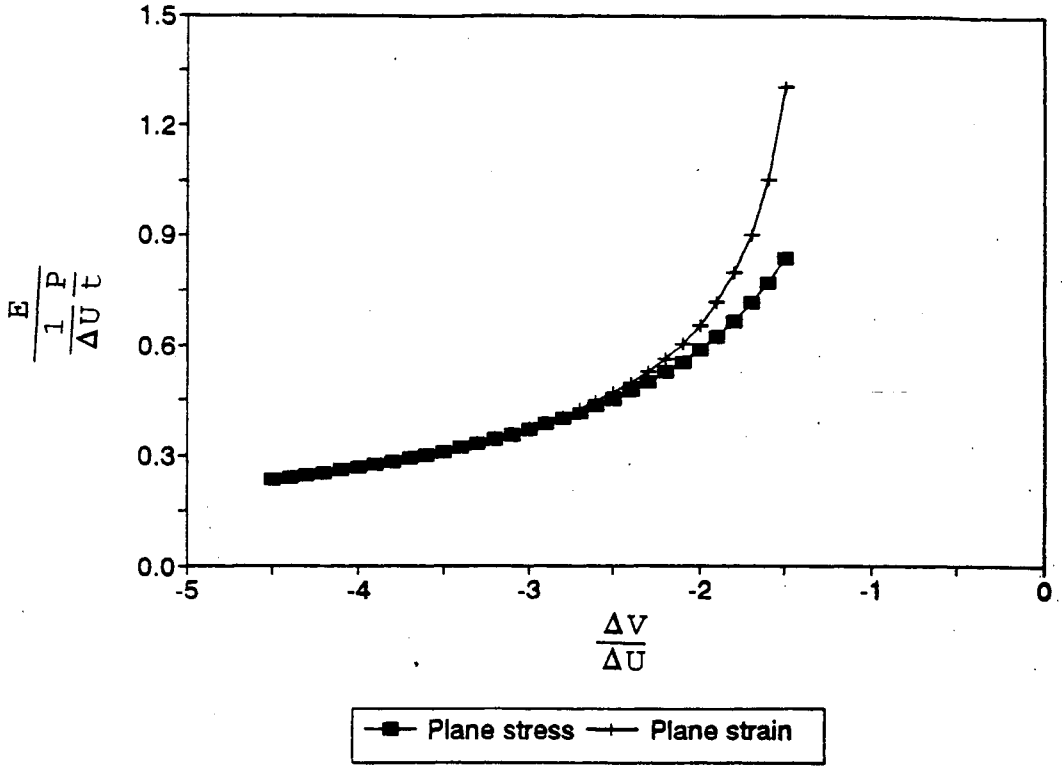

Figure A-9. Young's Modulus Versus ΔV/ΔU

Permanent Deformation

The characteristics of permanent deformation of asphalt concrete is evaluated by conducting the uniaxial or triaxial static creep test (22). Different rheology models have been developed to simulate the creep process. Burgers' model is a simple model which can be used to trace the creep up to the secondary stage (23).

Burgers' model is also known as the four constants linear viscoelastic model (Figure A-10). The constitutive equation for Burgers' model can be derived as follows:

$$\begin{aligned} \sigma &= E_1\epsilon_1 + \eta_1\frac{d\epsilon_1}{dt} \\ \sigma &= E_2\epsilon_2 \\ \sigma &= \eta_2\frac{d\epsilon_3}{dt} \\ \epsilon_i(0) &= 0 \quad (i=1,2,3) \end{aligned} \tag{A-29}$$

Take a Laplace transformation for the first equation

$$E_1\mathcal{L}(\epsilon_1)+\eta_1[s\mathcal{L}(\epsilon_1)-\epsilon_1(0)] = \sigma\frac{1}{s} \tag{A-30}$$

rearrange

$$\mathcal{L}(\epsilon_1) = \frac{\sigma}{\eta_1}\frac{1}{s}\frac{1}{s+\frac{E_1}{\eta_1}} = \frac{\sigma}{E_1}\left(\frac{1}{s}-\frac{1}{s+\frac{E_1}{\eta_1}}\right) \tag{A-31}$$

Take a back Laplace transformation

$$\epsilon_1(t) = \frac{\sigma}{E_1}(1-e^{\frac{E_1}{\eta_1}t}) \tag{A-32}$$

Solving the second and the third equation of (A-29),

$$\epsilon_2(t) = \frac{\sigma}{E_2}$$
$$\epsilon_3(t) = \frac{\sigma}{\eta_2}t \tag{A-33}$$

Therefore

$$\epsilon(t) = \epsilon_1(t)+\epsilon_2(t)+\epsilon_3(t) = \frac{\sigma}{E_1}(1-e^{-\frac{E_1}{\eta_1}t})+\frac{\sigma}{E_2}+\frac{\sigma}{\eta_2}t \tag{A-34}$$

Figure A-11 shows the typical strain - time relationship. It can be seen that $\epsilon_1(t)$, $\epsilon_2(t)$, and $\epsilon_3(t)$ represent the viscoelastic, elastic, and the viscous strains respectively.

The creep compliance J(t) and the creep modulus E(t) are defined as:

$$J(t) = \frac{\epsilon(t)}{\sigma}$$
$$E(t) = \frac{\sigma}{\epsilon(t)} \tag{A-35}$$

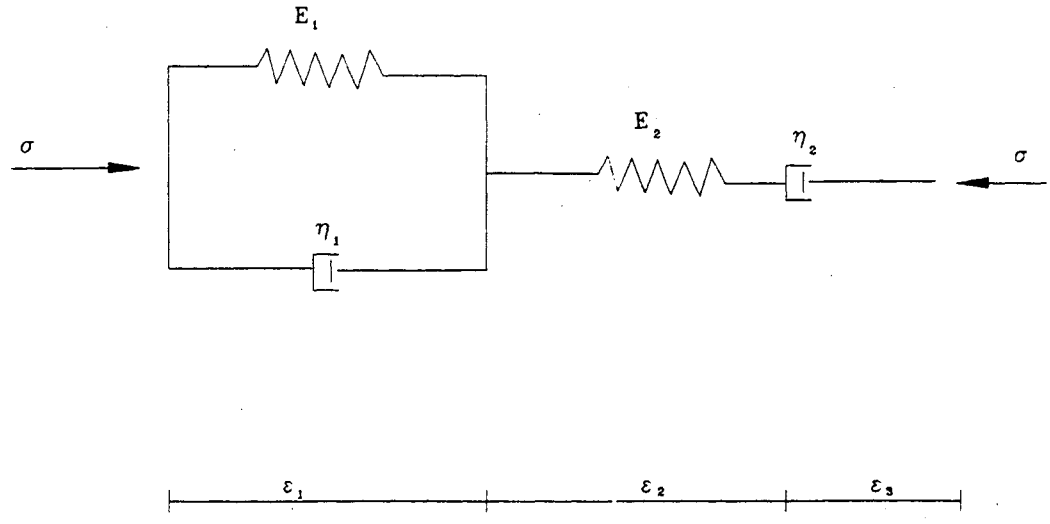

Figure A-10. Burgers' Model (four constants linear viscoelastic model) (23)

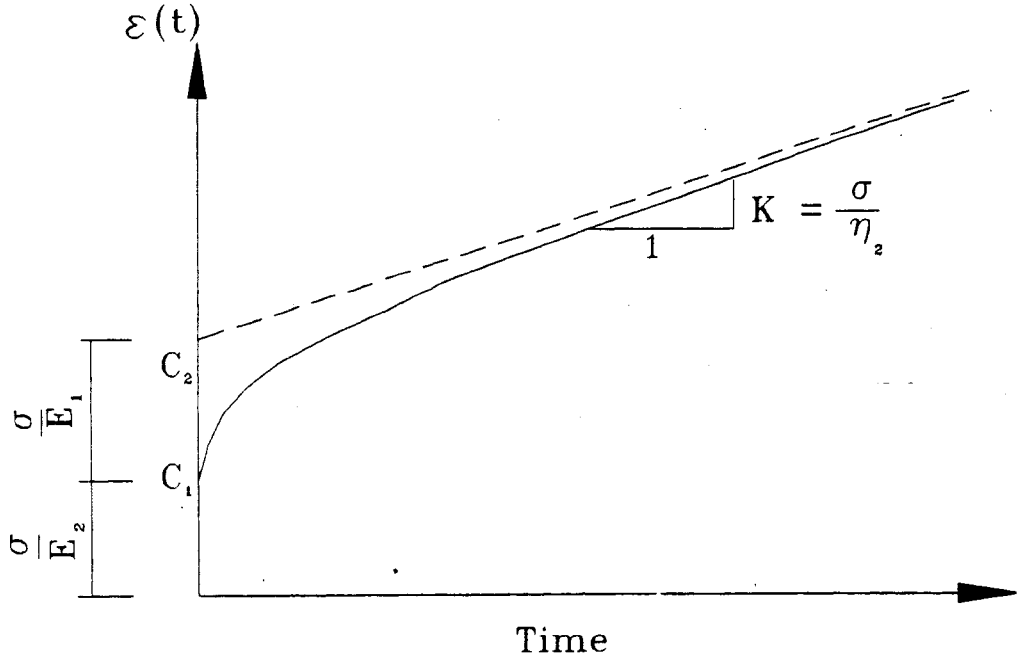

Figure A-11. Typical Creep Curve (23)

In the static creep test, the applied stress σ is held constant while the axial strain is measured. The creep compliance and creep modulus can be determined. If a constitutive model such as the Burgers's model is used to fit the experimental data, then the four parameters can be determined as follows:

1. Plot the strain versus time relationship according to the data.
2. Mark the intersection point C1 on the Y-axis, the coordinate of C1 is the instantaneous elastic strain $\epsilon(0)$, and calculate

$$E_2 = \frac{\sigma}{\epsilon(0)} \tag{A-36}$$

3. Draw a straight line that is tangent to the end of the secondary creep portion. Measure the slope K of this line, and calculate

$$\eta_2 = \frac{\sigma}{K} \tag{A-37}$$

Now the outline of the creep curve up to the secondary stage has been captured.

4. Extend the straight line drawn in step 3 all the way to the Y-axis. Mark the intersection point as C2. The coordinate difference between C1 and C2 represent the ultimate viscoelastic strain. So E_1 can be determined as

$$E_1 = \frac{\sigma}{C2-C1} \tag{A-38}$$

5. Use trial and error to vary η_1 until the plot can smoothly fit the curved part.